Preprints.org

Hypothesis

Not peer-reviewed version

The Biological Reboot: How the Alpha-Type-1 Polarized Dendritic Cell Restores Bidirectional Immune Instruction

Andrew Caravello * and Andrew Blidy

Posted Date: 15 April 2026

doi: 10.20944/preprints202604.0868.v2

Keywords: dendritic cell; IRF8; STAT3; bilateral disarmament; IL-12p70; immunosenescence; epigenetic reprogramming; mitochondrial fitness

Preprints.org is a free multidisciplinary platform providing preprint service that is dedicated to making early versions of research outputs permanently available and citable. Preprints posted at Preprints.org appear in Web of Science, Crossref, Google Scholar, Scilit, Europe PMC.

Copyright: This open access article is published under a Creative Commons CC BY 4.0 license, which permit the free download, distribution, and reuse, provided that the author and preprint are cited in any reuse.

Preprints.org (www.preprints.org) | NOT PEER-REVIEWED | Posted: 15 April 2026 doi:10.20944/preprints202604.0868.v2

Disclaimer/Publisher's Note: The statements, opinions, and data contained in all publications are solely those of the individual author(s) and contributor(s) and not of MDPI and/or the editor(s). MDPI and/or the editor(s) disclaim responsibility for any injury to people or property resulting from any ideas, methods, instructions, or products referred to in the content.

Hypothesis

The Biological Reboot: How the Alpha-Type-1 Polarized Dendritic Cell Restores Bidirectional Immune Instruction

Andrew Caravello [1,*] and Andrew Blidy [2]

[1] Independent Researcher, Medford, NJ, USA

[2] SaltusBiotech CSO, Pleasanton, CA, USA

* Correspondence: andrewcaravello@gmail.com

Abstract

Background: The dendritic cell initiates and directs antigen-specific immunity. Three Nobel Prizes frame the system it controls: Steinman (2011) for the dendritic cell as conductor of adaptive immunity; Allison and Honjo (2018) for CTLA-4 and PD-1 checkpoint inhibition; Sakaguchi, Brunkow, and Ramsdell (2025) for Foxp3+ regulatory T cell tolerance. **Hypothesis:** The evidence reviewed here establishes that these discoveries describe a single bidirectional circuit with the dendritic cell as its fulcrum, and that the tolerogenic default observed in aging, cancer, chronic infection, and senescence represents a correctable failure of dendritic cell instruction driven by a specific molecular chain: SASP–STAT3–DNMT/EZH2–IRF8 silencing. SASP cytokines activate STAT3 in hematopoietic progenitors; STAT3 recruits DNMT1/DNMT3B and EZH2 to silence IRF8 through dual DNA and histone methylation; IRF8 silencing—locked by a BATF3-dependent bistable switch with no stable intermediate within any given lineage, though different lineages have different switching thresholds producing the dose-dependent phenotypes in human IRF8 mutations (90)—simultaneously eliminates IL-12 transcription, disarms target cells against apoptosis, collapses genome surveillance, and installs bilateral disarmament across the immune synapse. STAT3 in parallel drives PD-L1 transcription on tolerogenic DCs and tumor cells. Six molecular locks on IL-12 operate at transcriptional initiation, elongation, post-translational, progenitor fate, biosynthetic, and Polycomb/histone methylation levels, with a seventh lock—the PGE2 chromatin trap—permanently closing the IL-12p35 locus through cAMP-dependent nucleosome stabilization during the maturation window. Seven self-reinforcing loops—including the SOCS3 feed-forward loop, the alpha-ketoglutarate trap blocking TET demethylases, the NAD+/SIRT1 acetylation lock, lactate-derived lysine lactylation, the STAT3-EZH2 Polycomb loop, and the mTOR-STAT3 amplification loop—ensure the tolerogenic default is metabolically as well as epigenetically locked. **Proposed correction:** The alpha-type-1 polarized dendritic cell (alpha-DC1), manufactured ex vivo with IFN-γ and multi-TLR engagement, escapes this architecture because its maturation commitment occurs outside the STAT3 field. It initiates a self-amplifying four-phase cascade that progressively restores IRF8 expression across the immune surveillance network, simultaneously re-enabling all ten IRF8-dependent surveillance functions, breaking all seven feedback loops by removing their SASP input, and reversing all three dimensions of bilateral disarmament through a single manufactured cell that renders itself unnecessary by correcting the upstream cause of its own requirement. **Significance:** This framework redefines the alpha-DC1 from an immunotherapy to a biological senolytic—an intervention that clears senescent cells by restoring the immune system's endogenous capacity to clear them—and redefines the therapeutic target from the effector compartment to the instructor.

Keywords: dendritic cell; IRF8; STAT3; bilateral disarmament; IL-12p70; immunosenescence; epigenetic reprogramming; mitochondrial fitness

© 2026 by the author(s). Distributed under a Creative Commons CC BY license.

Preprints.org (www.preprints.org) | NOT PEER-REVIEWED | Posted: 15 April 2026 doi:10.20944/preprints202604.0868.v2

1. Introduction

Every year, millions die from conditions sharing an upstream cause their physicians never measure. The grandmother whose cognition dims, the grandfather whose latent tuberculosis reactivates, the patient whose pancreatic cancer escapes checkpoint immunotherapy—each specialist treats the organ. None assesses the instructional state of the immune system that, had it been functioning, would have prevented the disease.

In 1973, Steinman and Cohn identified the dendritic cell [1]. Over two decades, Steinman demonstrated it was 100-fold more potent at initiating immunity than any other cell [2]. Hawiger proved the critical principle in 2001: without maturation, the DC delivers tolerance; with maturation, robust immunity [3]. The same cell, the same antigen, opposite outcomes. The DC makes a binary decision at each encounter: pathological or self?

Three Nobel Prizes converge on this fulcrum. Allison showed that CTLA-4 and CD28 integrate opposing signals from shared ligands [4], and blocking CTLA-4 caused complete tumor rejection [5]. Honjo identified PD-1 as a second brake. Both checkpoints trace to the DC: CTLA-4 competes for DC-provided costimulation, and PD-L1 is upregulated on immature DCs. Sakaguchi identified CD4+CD25+ regulatory T cells maintaining self-tolerance [6]—the CD25+ population first detected by Jackson, Blidy, and colleagues in 1990 [22]—with Foxp3 as their master transcription factor [7]. Wing showed CTLA-4 is essential for Treg suppression [8]; Qureshi showed Tregs physically capture CD80/CD86 from DCs through trans-endocytosis [9]; Kennedy showed CD86 is the primary sustained target [10]. The brake Allison identified is the weapon Sakaguchi's Tregs use to disarm the DC. One circuit, one fulcrum. This article proposes that the bidirectional discrimination Hawiger demonstrated is the fundamental organizing principle of adaptive immunity, that its failure explains the tolerogenic default across aging, cancer, chronic infection, and senescence, and that a defined ex vivo manufacturing protocol can restore it. This model explains why checkpoint blockade fails in the majority of patients: it releases inhibitory signals on effector T cells that were never properly instructed, directed against target cells armored against the killing mechanisms those T cells would use. It explains why vaccines fail in the elderly: the DCs that should convert antigen exposure into protective immunity have lost the IL-12 program encoding the instruction. And it explains why no single-target therapy has succeeded against age-related immune decline: the failure is not in one pathway but in the upstream instructor governing all of them.

2. The Tolerogenic Default: The Complete Mechanism

2.1. The Upstream Cause

Senescent cells accumulate with age and secrete the SASP—IL-6, G-CSF, IL-1β, PGE2, TGF-β [23]—activating STAT3 in HSCs through JAK1-JAK2/gp130 signaling. Chronic elevated cortisol co-activates STAT3 through glucocorticoid receptor co-occupancy, SOCS3 suppression, and C/EBPβ induction driving emergency myelopoiesis [24]. In cDC1s specifically, endogenous glucocorticoids constitutively suppress IL-12 production, amplified by 11β-HSD1 making cDC1s uniquely vulnerable to neuroendocrine suppression [109,110]. The bone marrow shifts to myeloid-biased output, expanding the MDSC compartment while contracting lymphoid progenitors [27]. Park showed IL-6/STAT3 directly regulates DC differentiation, producing DCs with impaired IL-12 and T cell priming [25].

The cellular SASP source is now identified. Doolittle showed in the JCI (2026) that bone marrow mesenchymal stromal cells display a profound senotype with full SASP, while myeloid cells develop only partial senescence and escape senolytic clearance within 96 hours [163]. The molecular switch is YAP/TAZ: mesenchymal cells possess active YAP/TAZ that declines with age, triggering cGAS-STING and full SASP; macrophages lack YAP expression and cannot enter canonical senescence [164,165]. Ambrosi confirmed that young HSCs in aged stroma produce myeloid skewing while the same cells in young stroma produce balanced output [166]. Mitchell showed IL-1β from the damaged

© 2026 by the author(s). Distributed under a Creative Commons CC BY license.

Preprints.org (www.preprints.org) | NOT PEER-REVIEWED | Posted: 15 April 2026 doi:10.20944/preprints202604.0868.v2

endosteum drives chronic emergency myelopoiesis in aged marrow [167]. The architecture is a two-step relay: senescent mesenchymal cells produce the SASP; the SASP acts on myeloid progenitors through the STAT3 axis.

2.2. The Silencing Event

STAT3 performs one molecular event producing every downstream failure. It induces DNMT1 through GAS/SIE elements in the DNMT1 promoter and upregulates DNMT3B, which methylate the IRF8 promoter [33,92]. Simultaneously, STAT3 transcriptionally induces EZH2 by binding its promoter [176] and physically complexes with EZH2, DNMT1, and HDAC1 [51,177], creating a dual-mark silencing event: DNA methylation by DNMTs and H3K27me3 by EZH2, reinforced by histone deacetylation. EZH2 methylates STAT3 at K49 and K180, enhancing STAT3 activity [178,179], creating a fifth self-reinforcing loop. Fang demonstrated EZH2 recruitment to the IRF8 promoter deposits H3K27me3 and downregulates IRF8 in myeloid-lineage cells [175]. The IRF8 promoter is bivalently marked (H3K27me3/H3K4me3) in HSCs [180]—precisely the substrate for age-associated hypermethylation—explaining why the tolerogenic default is age-dependent but not purely age-determined.

IRF8 is not merely a lineage factor. It is a single transcription factor deployed across every cell type in the immune surveillance network, whose silencing produces coordinated multi-system failure. Its functions span ten domains at once.

As the **instructor**, IRF8 synergistically activates IL-12p35 transcription with IRF1 and is absolutely required for IL-12p40 production [62]. IRF8 is also a terminal selector of the cDC1 lineage: it is required not just for initial development but for ongoing survival, such that deleting IRF8 in a committed cDC1 induces complete transcriptional, functional, and epigenetic reprogramming into a cDC2 [63]. The identity is actively sustained by continuous IRF8 expression—not passively maintained.

As the **executioner**, IRF8 directly controls five independent apoptotic pathways: it represses BCL-2, overriding chemotherapy resistance [64]; represses FLIP, the caspase-8 inhibitor blocking both FasL and TRAIL-mediated death—nuclear IRF8 was absent in 92% of human soft tissue sarcomas while 99% expressed FLIP [65]; regulates acid ceramidase for Fas-dependent apoptosis [66]; activates Bax transcription in primary myeloid cells [67]; and represses PTPN13/Fap-1, the Fas-associated phosphatase inhibiting Fas-induced apoptosis [68]. IRF8 does not sensitize the cell to one form of death. It installs apoptotic competence across every available pathway.

As the **gatekeeper**, IRF8 physically interacts with C/EBPα and prevents its chromatin binding in monocyte-DC progenitors, blocking the neutrophil and MDSC differentiation program [69]. When STAT3 silences IRF8, C/EBPα drives MDSC expansion unopposed. Breast and pancreatic cancers exploit this mechanism systemically by producing G-CSF that downregulates IRF8 in bone marrow progenitors [71].

As the **danger sensor**, IRF8 physically associates with STING upon DNA damage in a transcription-independent role, serving as a scaffold essential for STING polymerization and TBK1-mediated phosphorylation; IRF8 deficiency blocks DNA damage-induced cellular senescence signaling [74]. The checkpoint is absolute: without phospho-IRF8(S151), DCs can import cGAMP normally and STING dimerizes normally, but polymerization—the step required for IRF3 activation and IFN-β production—fails entirely [74]. This means radiation-generated or SASP-generated cytoplasmic DNA activates cGAS, produces cGAMP, and the signal dead-ends at STING dimerization in every IRF8-silenced DC. The alpha-DC1, with restored IRF8, is therefore prerequisite—not merely additive—to any intervention that generates STING-activating signals. Without IRF8, damaged cells accumulate without activating the danger signals that would mark them for clearance. IRF8 also enables crosstalk between TLR and IFN-γ signaling through TRAF6 interaction, meaning IRF8 loss disables both pathogen detection and IFN-γ amplification [75].

IRF8 additionally operates as: **effector differentiator** (required for CD8+ T cell naïve-to-effector transition and 3D chromatin reorganization maintaining antitumor activity [72,73]); **tissue sentinel**

© 2026 by the author(s). Distributed under a Creative Commons CC BY license.

Preprints.org (www.preprints.org) | NOT PEER-REVIEWED | Posted: 15 April 2026 doi:10.20944/preprints202604.0868.v2

(defines microglial epigenetic landscape; drives mucosal IFN-γ in gastric epithelium [76,77]); **autophagy director** (activates autophagosome formation; deficiency blocks senescent cell debris processing [78]); **genome guardian** (indispensable for PML bodies and FANCF DNA repair [30,31]); **NK cell orchestrator** (controls Zbtb32 through IL-12/STAT4; biallelic mutations cause familial NK deficiency [79,80]); and **pathogen destroyer** (activates Nramp1/SLC11A1 and GBP/IRG families for intraphagosomal killing [81,82]). When IRF8 is silenced, all ten functions collapse from one epigenetic event. This is not ten separate failures. It is one failure expressed across every cell type in the immune surveillance network. While multiple transcriptional programs contribute to immune regulation, the convergence of developmental, functional, and genetic evidence identifies IRF8 as a non-substitutable node within this system, rather than one of several redundant regulators. Other transcriptional regulators contribute to individual domains, but no alternative node reproduces the coordinated ten-domain collapse observed with IRF8 silencing.

Ibrahim demonstrated the complete chain: MDSC-derived IL-10 activates STAT3, STAT3 binds DNMT1/DNMT3B promoters, DNMTs methylate IRF8, with human colorectal carcinomas showing higher DNMT and lower IRF8 than normal tissue [33]. McGough showed the lock: methylation recruits MBD1/PIAS1 that blocks STAT1 access, rendering the locus unresponsive to IFN-γ [34]. The NFIL3-dependent super-enhancer cascade maintaining IRF8 is strictly cis-dependent, vulnerable to upstream perturbation [83]. IRF8 autoactivates through a BATF3-dependent super-enhancer [141], creating a bistable system with two stable states: IRF8-high (surveillance) and IRF8-off (tolerogenic). No stable intermediate exists. STAT3 activation is graded, accumulating over years; but the IRF8 switch is binary—a slow dimmer drives a sudden toggle.

Two mechanisms accelerate collapse at different stages. In progenitors, IL-6-elevated C/EBPβ outcompetes NFIL3 at Zeb2 enhancer binding sites, blocking cDC1 specification at the developmental stage where FLT3L normally reinforces IRF8 through cell division [70,111,112,169]. In committed cells, STAT3-driven DNMT silences IRF8 directly, with acetylated STAT3 escorting DNMT1 to target promoters [113] while the MBD1/PIAS1 complex excludes both STAT1 and TET enzymes [34]. The clinical consequence is that a macrophage or DC without IRF8 is alive, metabolically active, and present in the tissue, but functionally deaf and blind to the pathology occurring around it. It cannot sense pathogens through the TLR/NLR apparatus IRF8 controls, cannot process antigens through the MHC machinery IRF8 coordinates, cannot kill through the phagosome maturation pathways IRF8 governs, and cannot recruit help through the chemokines IRF8 induces [32]. The cell is present. The perceptual apparatus that would make its presence meaningful has been erased.

Independent evidence establishes mitochondrial fitness as a critical determinant of cDC1 function. You and colleagues identified metabolically distinct cDC1 subsets: $[TMRM/MG]^{hi}$ cells with high OXPHOS and enhanced antigen presentation versus $[TMRM/MG]^{lo}$ cells with depolarized mitochondria and impaired priming, with the fit subset declining during tumor progression [143]. OPA1 acting through NRF1 maintained the electron transport chain; OPA1 deletion depolarized mitochondria and activated AMPK-dependent autophagy degrading MHC-I from the cDC1 surface [143,144]. Molina and Haldar confirmed this in Science (2026): intratumoral cDC1 mitochondrial membrane potential declines progressively during tumor progression [168]. The framework provides the answer You and colleagues left unresolved: the same SASP-STAT3 field that silences IRF8 creates the metabolic environment degrading mitochondrial fitness. IRF8 silencing eliminates cDC1 identity itself—converting cDC1s to cDC2s lacking the Mst1/2-maintained oxidative program specific to cDC1s [145].

2.3. The Seven Locks on IL-12

STAT3 installs seven molecular locks on IL-12, each at a different level. **Lock 1:** STAT3 blocks c-Rel recruitment to IL-12p40 [54]. **Lock 2:** STAT3 excludes CDK9/P-TEFb from the IL-12p35 elongation complex [50]. **Lock 3:** IL-6-induced arginase-1 and cathepsin L degrade IL-12 post-translationally [35]. **Lock 4:** STAT3/C/EBPβ suppresses MLL1 through miRNAs, arresting myeloid maturation entirely [56]. **Lock 5:** Mitochondrial depolarization imposes a biosynthetic lock—Mst1/2-maintained

© 2026 by the author(s). Distributed under a Creative Commons CC BY license.

Preprints.org (www.preprints.org) | NOT PEER-REVIEWED | Posted: 15 April 2026 doi:10.20944/preprints202604.0868.v2

OXPHOS is required for IL-12 in cDC1s [145]; when mitochondria depolarize, citrate export collapses, shutting down the ER/Golgi membrane expansion required for IL-12 secretion [154]. AMPK activation following ATP depletion further blocks the glycolytic switch TLR-stimulated DCs require [146]. IL-12p70 requires continuous synthesis and vesicular export; mitochondrial depolarization eliminates IL-12 before degrading MHC-I, meaning depolarized cDC1s write tolerance at every cross-presentation event. Kalinski demonstrated that DCs matured with PGE2 permanently lose IL-12p70 competence [26]; the positioned nucleosome at IL-12p35 must be remodeled within 24 hours or the locus is permanently silenced [29]. **Lock 6:** PRC2/EZH2-mediated H3K27me2 directly at IL-12 promoters—Wen showed post-sepsis DCs exhibit stable decreased H3K4me3 and increased H3K27me2 with PRC2 remaining bound, persisting at least six weeks [181]; DiNardo elevated this as paradigmatic epigenetic scarring in the NEJM [182]. Critically, Zhan showed PRC2-mediated repression is dispensable for normal DC homeostasis [183], indicating EZH2's role is pathological STAT3 redirection, not developmental function. Lock 7: The PGE2 chromatin trap—PGE2 through EP2/EP4 → cAMP → PKA stabilizes the positioned nucleosome at IL-12p35 during the maturation window; once closed, even IFN-γ cannot reopen it [238,239]. Kalinski demonstrated the irreversibility directly: differences in IL-12 capacity established during final maturation are stable after PGE2 removal, and fully mature DCs become unsusceptible to further modulation [239]. PGE2 simultaneously shifts the IL-12/IL-23 balance by suppressing p35 while upregulating p19, actively redirecting immunity toward Th17 [240], and destroys NK-DC crosstalk by suppressing CCL5, CCL19, and CXCL10 in a cAMP-dependent manner imprinted during maturation [241]. Critically, Bayerl and colleagues demonstrated in Immunity (2023) that tumor-derived PGE2 programs cDC1 dysfunction through a mechanism dependent on IRF8 loss—providing a second SASP-derived route to IRF8 silencing (PGE2 → cAMP → IRF8 loss) independent of the STAT3 → DNMT epigenetic route, both converging on the same bilateral disarmament [242]. Blockade of PGE2-EP2/EP4-cDC1 axis prevented dysfunction and reinvigorated anti-cancer CD8+ T cell responses [242]. Because senescent cells constitutively produce PGE2 through COX-2 upregulation, every endogenous DC encountering the SASP during its maturation window has the IL-12p35 locus permanently closed—the PGE2 trap is the fail-safe ensuring the tolerogenic default cannot be escaped from within the system.

2.4. Bilateral Disarmament

The same STAT3-DNMT event that silences IRF8 in immune cells simultaneously armors target cells. IRF8 methylation de-represses BCL-2, accumulates FLIP, silences Bax, and de-represses Fap-1—five antiapoptotic mechanisms [30,31]. The immune system cannot attack (lost IL-12-competent DCs, effector differentiation, NK activation). Targets cannot be killed (antiapoptotic armor). Mitochondrial collapse provides parallel immune-side disarmament through AMPK-dependent MHC-I degradation in surviving cDC1s [143,144]. STAT3 activation also blocks autophagy in DCs through LC3-II reduction and p62 accumulation, reversible by STAT3 inhibition [204]—disabling the autophagosome formation that IRF8 normally directs [78] and preventing senescent cell debris processing. The SASP-driven oxidative environment creates a further vulnerability: DCs themselves undergo ferroptosis from lipid peroxidation, losing MHC-I expression and all instructional capacity [233,234]—and IRF8's control of acid ceramidase [66] may be the protective mechanism lost when IRF8 is silenced, rendering DCs ferroptosis-susceptible. Beyond ferroptosis itself, the oxidized phospholipids generated by ACSL4-dependent lipid peroxidation suppress IL-12 through inhibition of histone H3 phosphorylation even in surviving DCs, creating an additional barrier to IL-12 production independent of IRF8 methylation status. Ceramide metabolism operates on both sides of the immune synapse: in target cells, IRF8-controlled ceramidase regulates Fas-dependent apoptosis; in DCs, ceramide accumulation through acid sphingomyelinase is required for full maturation and IL-12 production—and sphingosine-1-phosphate (S1P), which accumulates in the aging microenvironment, actively suppresses DC IL-12 while promoting target cell survival [236]. STAT3 adds PD-L1 transcription on both tolerogenic DCs and tumor cells [158–160]. This is bilateral

© 2026 by the author(s). Distributed under a Creative Commons CC BY license.

Preprints.org (www.preprints.org) | NOT PEER-REVIEWED | Posted: 15 April 2026 doi:10.20944/preprints202604.0868.v2

disarmament (Figure 1). It explains why checkpoint blockade fails in the majority: releasing brakes on T cells never properly instructed, aimed at armored targets, addresses neither side.

Figure 1. The SASP-STAT3-DNMT/EZH2-IRF8 Silencing Chain and Bilateral Disarmament

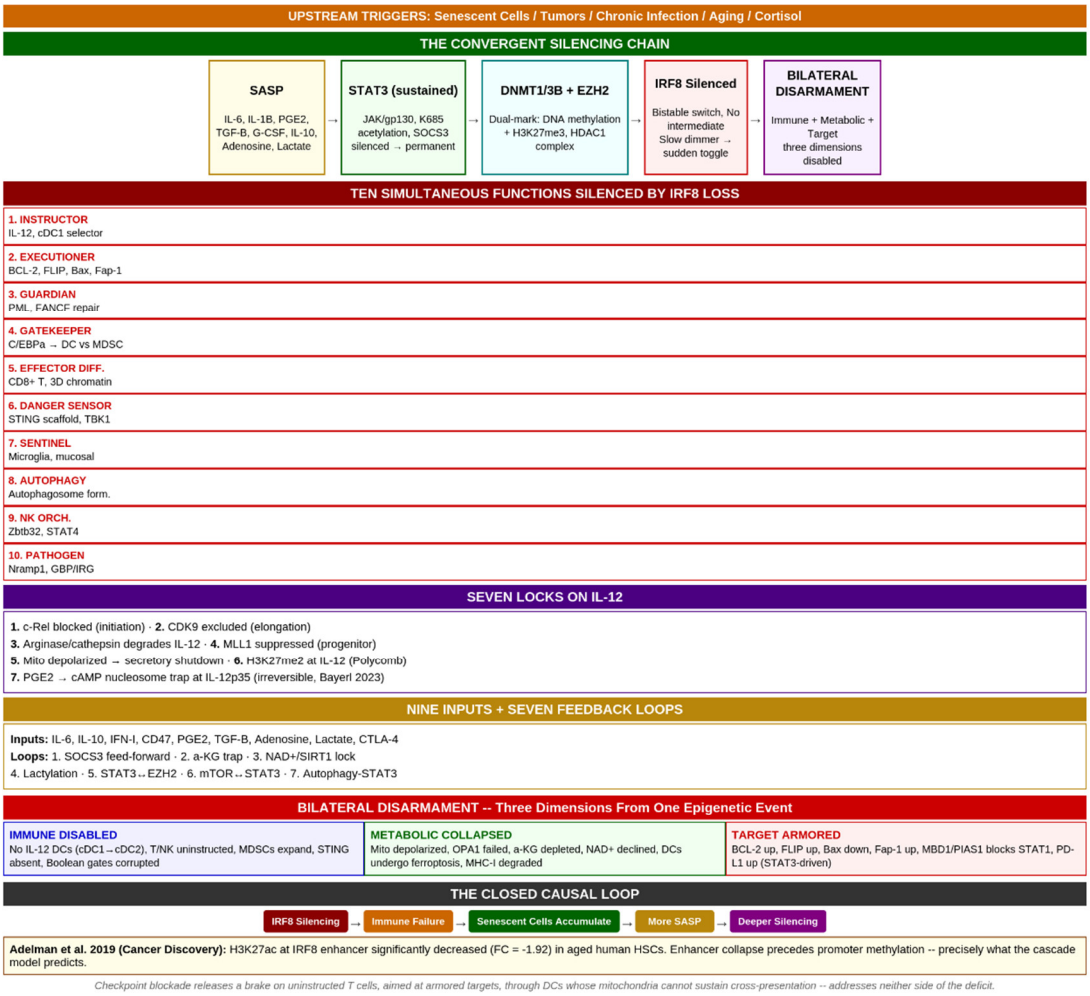

Figure 1. The SASP–STAT3–DNMT/EZH2–IRF8 silencing chain and bilateral disarmament. SASP cytokines activate STAT3 in hematopoietic progenitors, inducing DNMT1/DNMT3B and EZH2 to methylate the IRF8 promoter through dual DNA and histone methylation. A BATF3-dependent autoactivation loop creates a bistable switch: once methylation crosses the threshold, IRF8 collapses with no stable intermediate [141]. IRF8 silencing simultaneously collapses ten surveillance functions while armoring target cells against killing. Nine self-reinforcing inputs lock the system, including a SOCS3 feed-forward loop, CTLA-4 reverse signaling activating STAT3 [95], and STAT3-driven PD-L1 transcription [158]. Seven locks on IL-12 operate at transcriptional initiation, elongation, post-translational, progenitor fate, biosynthetic, Polycomb/histone methylation, and PGE2 chromatin trap levels. Seven metabolic-epigenetic feedback loops—SOCS3 feed-forward, NAD+/SIRT1 acetylation lock, alpha-ketoglutarate trap, lactate-derived lysine lactylation, the STAT3-EZH2 Polycomb loop, and the mTOR-STAT3 amplification loop—ensure the default is metabolically as well as epigenetically locked. The closed causal loop is shown: IRF8 silencing produces immune failure that allows senescent cell accumulation, generating more SASP that deepens silencing [195,196]. Direct epigenomic evidence from Adelman et al. [189] confirms significant H3K27ac loss at the IRF8 enhancer in aged human HSCs.

2.5. The Self-Reinforcing Architecture

The tolerogenic default is self-reinforcing because its output maintains its input. Nine inputs converge on STAT3 directly or through autocrine cytokine intermediaries: IL-6, IL-10, chronic type I IFN, CD47/SIRPα, PGE2, TGF-β, adenosine, lactate, and CTLA-4 reverse signaling on DCs [95]. The CD47 input is bidirectional: STAT3 directly binds the CD47 promoter and drives its transcription in

© 2026 by the author(s). Distributed under a Creative Commons CC BY license.

Preprints.org (www.preprints.org) | NOT PEER-REVIEWED | Posted: 15 April 2026 doi:10.20944/preprints202604.0868.v2

tumor cells, while CD47 engagement of SIRPα on APCs activates STAT3 in the APC—creating a feedforward amplification loop. STAT3 inhibition simultaneously reduces the CD47 don't-eat-me signal and increases surface calreticulin (the eat-me signal) through ER stress, producing a dual phagocytic shift on a single target. The adenosine input is itself STAT3-dependent: STAT3 upregulates CD73, the ectoenzyme generating adenosine from AMP, and adenosine signals through A2AR/A2BR on DCs to suppress IL-12 while inducing IL-10, TGF-β, and IDO [237]—creating a self-reinforcing purinergic loop that the alpha-DC1's ex vivo bioreactor breaks by removing the extracellular ATP substrate entirely. IL-12-deficient DCs expand Tregs because they deliver antigen without the polarizing signal that would generate effectors. Tregs strip remaining DCs of costimulatory molecules through CTLA-4 trans-endocytosis [9], and CTLA-4 engagement on DCs concurrently activates STAT3 phosphorylation suppressing NF-κB activity and CD80/CD86 transcription [95]—a dual mechanism physically removing costimulatory molecules while preventing their re-expression. MDSCs expand Tregs through arginase, IDO, TGF-β, and IL-10 [27]. IDO-expressing DCs generate kynurenine activating AhR in an autocrine maintenance loop. Regulatory B cells produce IL-10 and IL-35, competing with IL-12 at IL-12Rβ2. The Wnt/beta-catenin brake is removed, enabling tolerogenic signaling [28]. Osteopontin is de-repressed from IRF8 silencing, creating a soluble T cell checkpoint. The IRF4/IRF8 balance shifts toward IRF4 dominance, breaching B cell anergy and degrading antibody quality from germinal center maturation to low-affinity plasmablast differentiation [36]. NFATc1 is de-repressed, driving pathological osteoclastogenesis degrading the bone marrow niche [37].

Seven self-reinforcing loops lock the system (Figure 4). **Loop 1 (SOCS3 feed-forward):** STAT3 induces DNMT1, which methylates the SOCS3 promoter, silencing the negative feedback brake that normally terminates STAT3 within two hours; SOCS3 methylation rates reach 60% in AML marrow versus zero in remission [114,115]. **Loop 2 (α-KG trap):** TET demethylases, the only enzymes capable of reversing IRF8 methylation, require α-ketoglutarate as obligate cofactor [147]. When mitochondria depolarize, α-KG drops while succinate and fumarate—competitive TET inhibitors with IC50 values of approximately 550 and 400 μM respectively—accumulate [148]. Liu demonstrated the α-KG/succinate ratio directly controls TET2-dependent reprogramming in macrophages [149]; Zhou traced the complete chain from mitochondrial respiration through glutaminolysis-derived α-KG to TET2-mediated DNA hydroxymethylation in myeloid cells [150]. D-2-HG and L-2-HG inhibit IL-12 secretion in human DCs [155] and impair DC differentiation [156]. **Loop 3 (NAD+/SIRT1 lock):** SIRT1 removes K685 acetylation from STAT3 required for STAT3-DNMT1 complex formation [113]. Nie demonstrated that SIRT1 physically deacetylates STAT3 at K685, with resveratrol decreasing STAT3 acetylation in wild-type but not SIRT1-knockout mouse embryonic fibroblasts—genetic proof that SIRT1 is the obligate deacetylase [151]. SIRT1 is additionally vulnerable to covalent inactivation by 4-hydroxynonenal, a lipid peroxidation end-product that accumulates with age, meaning oxidative damage can disable this lock independently of NAD+ depletion. Limagne confirmed this in immune cells: resveratrol, metformin, and SRT1720 all reduced STAT3 K685 acetylation, with all effects abolished in CD4-specific SIRT1-knockout T cells [152]. When NAD+ declines with mitochondrial failure [153], SIRT1 cannot deacetylate STAT3, and the acetylated STAT3-DNMT1 complex methylates IRF8 unopposed. **Loop 4 (lactylation):** Tumor-derived lactate induces lysine lactylation (Kla), driving immunosuppressive gene programs in DCs [161]; lactate-induced ENSA-K63 lactylation activates STAT3/CCL2 signaling [162]. **Loop 5 (Polycomb):** STAT3 induces EZH2; EZH2 methylates STAT3 K49/K180 to enhance activity; enhanced STAT3 induces more EZH2 [176,178,179]—continuously reinforcing H3K27me3 alongside DNA methylation. **Loop 6 (mTOR amplification):** mTOR phosphorylates STAT3 at Ser727, required for maximal transcriptional activity including DNMT1 induction [206]; STAT3 reciprocally activates mTOR by suppressing the mTOR inhibitor REDD1 [207]—creating a bidirectional amplification loop. Rapamycin phenocopies key alpha-DC1 effects by promoting IL-12 via NF-κB while blocking IL-10 via STAT3 in DCs [208], but cannot replace the alpha-DC1 because chronic mTOR inhibition violates the pulsatile temporal code and cannot reverse IRF8 methylation already installed. Moreover, Zhao demonstrated in Blood that

© 2026 by the author(s). Distributed under a Creative Commons CC BY license.

Preprints.org (www.preprints.org) | NOT PEER-REVIEWED | Posted: 15 April 2026 doi:10.20944/preprints202604.0868.v2

mTOR directly controls IRF8 expression through a STAT5 axis: mTOR deficiency causes STAT5 overactivation, which downregulates IRF8 [232]—creating a pincer attack where STAT3 silences IRF8 epigenetically from one direction while STAT5 overactivation from chronic mTOR inhibition suppresses it transcriptionally from the other, explaining why acute mTOR inhibition is immunogenic but chronic mTOR inhibition becomes tolerogenic.

2.6. Six Lines of Convergent Proof

Six independent lines establish this mechanism as convergent fact. **First,** the defect is environmental: Lung showed elderly monocytes generate unimpaired DCs ex vivo [38]. **Second,** STAT3 is the specific cause: Zhou demonstrated in Nature (2025) that the STAT3/STAT5 balance determines DC functional fate, that STAT3 activation is entirely paracrine, and that cDC1-specific STAT3 knockout restored IL-12, MHC, and costimulatory molecules while reducing tumor growth [39]. **Third,** DNMT-mediated IRF8 silencing is the mechanism [33], now demonstrated in non-malignant systems: Waight showed SASP cytokines G-CSF/GM-CSF facilitated IRF8 downregulation via STAT3 in normal bone marrow progenitors, producing MDSC-like populations identical to those in tumor-bearing mice [197]; Harroch showed IL-6 directly and strongly downregulates IRF8 transcripts in myeloid cells [198]. **Fourth,** IL-12 deficiency is the clinical defect: age-associated decreases in TLR-stimulated DC IL-12 production specifically predicted poor influenza vaccine response [47], and frailty, not chronological age, correlated with decreased IL-12/23 production [48]. **Fifth,** correcting the DC alone suffices: Zhivaki demonstrated in Cell (2024) that correcting DC defects enabled CD4+ T cells to eradicate tumors in aged mice where PD-1 and CTLA-4 checkpoint therapies failed entirely [40]. **Sixth,** the framework predicts senolytic myeloid clearance should fail because myeloid cells are paracrine targets, not the senescence source—confirmed by Doolittle: p16+ myeloid cells cleared by senolysis repopulated within 96 hours because new progenitors re-encountered the STAT3 field from still-senescent mesenchymal cells [163]; and strikingly by Luo, who showed dasatinib plus quercetin promoted tumor progression by eliminating senescent cells while impairing immune surveillance [170]. These findings support a causal role for STAT3-driven epigenetic silencing within this framework, while remaining consistent with additional modulatory pathways operating in parallel.

This model draws a critical distinction from conventional immunosenescence. Standard models emphasize thymic involution and T cell repertoire contraction—real phenomena locating the deficit in the effector compartment. The hypothesis here locates the primary deficit upstream, at DC instruction. Guo confirmed directly: DC dysfunction in aged mice caused NK cell failure, but young DCs efficiently activated aged NK cells [49]. The effector compartment is intact—waiting for correct instruction. Stirewalt demonstrated IRF8 is the only gene with conserved age-associated decreases across both human and murine HSPCs [86]. Molony showed human monocytes from older adults fail to produce IRF8 in response to viral infection; knocking down IRF8 in younger adults replicated aged defects; restoring IRF8 in older adults restored IFN responses [55]. The Phase III DCVax-L data are consistent: patients with median age 56 and maximally immunosuppressive tumor microenvironments showed extended survival following DC vaccination [21]—if the deficit were in the effector compartment, DC vaccination in this population should fail. Hambleton provided the definitive human genetic proof: autosomal dominant IRF8 deficiency caused selective cDC1 depletion with IL-12 reduced to one-third of controls; autosomal recessive caused complete monocyte/DC absence plus myeloproliferative syndrome [90]. One gene, two dose-dependent phenotypes, the entire tolerogenic default encoded in a single locus.

3. The Alpha-DC1 as Restored Instructor

3.1. Manufacturing as Chromatin Programming

Correcting the tolerogenic default requires manufacturing a DC whose maturation occurs outside the STAT3 field. The alpha-DC1 protocol achieves this [11]. Patient monocytes collected by

© 2026 by the author(s). Distributed under a Creative Commons CC BY license.

Preprints.org (www.preprints.org) | NOT PEER-REVIEWED | Posted: 15 April 2026 doi:10.20944/preprints202604.0868.v2

leukapheresis carry the complete HLA repertoire. They are not broken. The defect is environmental, not cellular. Placed in a closed-system bioreactor with GM-CSF, the cell is severed from every paracrine STAT3 input at once: no IL-6 from senescent cells, no IL-10 from Tregs, no PGE2, no adenosine, no lactate. Without continuous STAT3 input, the STAT5 axis activated by GM-CSF proceeds without competitive inhibition, driving differentiation toward the DC lineage and opening the chromatin landscape at surveillance program enhancers.

The maturation cocktail—IFN-α, poly-I:C, TNF-α, IL-1β, and IFN-γ, excluding PGE2 and IL-6 [12]—is applied after differentiation completes. The PGE2 exclusion is not an empirical formulation choice but a mechanistic necessity: Bayerl demonstrated that PGE2 silences IRF8 in cDC1s through EP2/EP4 → cAMP signaling [242], meaning any PGE2 exposure during the maturation window would close the IL-12p35 locus before IRF8 induction could occur, producing phenotypically mature but instructionally dead DCs—the precise failure mode that characterized a generation of PGE2-containing DC vaccine protocols [243]. The alpha-DC1's ex vivo manufacturing escapes both the STAT3 → DNMT epigenetic route and the PGE2 → cAMP transcriptional route to IRF8 silencing simultaneously. BCG-derived components activateing TLR2/TLR4/TLR9/NOD2 in concert to produce a qualitatively different maturation state than any single TLR agonist [41]. Shankar demonstrated that IFN-γ added during BCG-induced maturation synergistically upregulates IL-12 while inhibiting IL-10 [42]. IFN-γ, the canonical inducer of IRF8 expression across all cell types [61], induces IRF8 through STAT1/IRF1; critically, IFN-γ must arrive during maturation, not differentiation. Rojas-Canales demonstrated that early IFN-γ produces tolerogenic DCs with suppressed CD83, CD80, and IL-12p70, while late IFN-γ produces immunogenic DCs [52]—the temporal code principle, where STAT3 occupancy of shared receptor phosphotyrosine motifs with STAT1 [106] determines how IFN-γ is read. Khateb showed a chromatin priming element in IRF8's third intron maintains a permissive state, overridden when silenced by STAT3-driven methylation [60]. Activation drives deSUMOylation through SENP1, switching IRF8 from repressor to activator [43]. The protocol produces DCs with 10–100× more IL-12p70 than tolerogenic DCs [12], with retained receptor-mediated uptake through DNGR-1/CLEC9A, CD64, and DEC-205 for cross-presentation [11,13].

Unlike approaches requiring exogenous transcription factor delivery, the alpha-DC1 exploits the endogenous PU.1/IRF8/BATF3 circuit already present in myeloid progenitors. No exogenous gene delivery is involved. The inventive principle is environmental: removing the progenitor from the STAT3 field before differentiation completes is sufficient. The ex vivo escape corrects both the epigenetic defect (IRF8 silencing) and the metabolic defect (mitochondrial depolarization): the alpha-DC1 differentiates outside SASP-driven metabolic stress, maintaining polarized OPA1-dependent mitochondria and high OXPHOS capacity characteristic of $[TMRM/MG]^{hi}$ cDC1s [143,144]. This dual correction cannot be achieved by IFN-γ alone: Tian showed IFN-γ enhances oxygen consumption through NAMPT-dependent NAD+ salvage but does not induce mitochondrial biogenesis [157]. Restoration of mitochondrially fit cDC1s in endogenous tissue therefore depends on Phase 4 emergence of new IRF8-competent progenitors whose developmental program—executed outside the SASP field—installs both chromatin state and metabolic architecture de novo.

© 2026 by the author(s). Distributed under a Creative Commons CC BY license.

Preprints.org (www.preprints.org) | NOT PEER-REVIEWED | Posted: 15 April 2026 doi:10.20944/preprints202604.0868.v2

3.2. Bidirectional Discrimination and Breaking the Tolerogenic Loop

The alpha-DC1 restores bidirectional capacity. Alpha-DC1-educated T cells overexpress DNAM-1 and NKG2D, creating dual-key selectivity: TCR recognition plus NK receptor stress ligand recognition [13]. IL-12 both sensitizes the TCR approximately 10-fold and enables TCR-independent killing through DNAM-1 stress ligand recognition—two mechanistically separate programs installed by the same signal [209]. IL-12 directly drives NKG2A expression recognizing HLA-E on healthy tissues—a primary IL-12 effect independent of IFN-γ [44,210]—and downregulates KIRs on NK cells for MHC-I-retaining target killing [89]. The DC programs AND gates (TCR + costimulation), phagosome-autonomous AND gates (antigen and TLR ligand must co-localize for presentation, as Blander and Medzhitov demonstrated [130]), dual-key AND gates (TCR + stress ligand), and NOT gates (NKG2A + HLA-E). The tolerogenic default corrupts every gate; the alpha-DC1 reinstalls the complete Boolean architecture from a clean copy.

The manufactured DC resists the tolerogenic feedback loop: NF-κB nuclear translocation installs costimulatory molecule replenishment faster than CTLA-4 trans-endocytosis strips them, and the IL-12 program was irreversibly locked before any CTLA-4 encounter. IL-12p70 converts Foxp3+ Tregs into IFN-γ-producing Th1 cells [14], converts regulatory B cells into IFN-γ effectors through STAT4/T-bet [87], reprograms tumor-associated macrophages within 90 minutes [88], and IFN-γ kills MDSCs through Bcl2a1 repression. Pulsatile delivery is ensured by perforin-dependent elimination of the DC by its own educated T cells [96,97], constraining IFN-γ exposure and preventing IDO installation at the 48–96 hour threshold [93,94,98]. IFN-γ-induced iNOS provides a bimodal brake: high NO suppresses IDO enzymatic activity and promotes its proteasomal degradation [116–119]. A third brake operates through the IRF8-IDO dependency itself. Orabona and colleagues demonstrated that IRF8 is required for IDO expression: silencing IRF8 in IDO-competent DCs abolished Indo mRNA and kynurenine production in both murine and human DCs [199]. Gargaro and colleagues confirmed that IDO1 transcription in mature cDC1s requires IRF8/BATF3 co-occupancy at an AICE element at −126 bp in the Ido1 promoter, with CRISPR validation, and that IDO-competent cDC1s use tryptophan catabolism to educate inflammatory cDC2s toward tolerance through L-kynurenine/AhR metabolic communication [200]. This creates a paradox the framework resolves: in the tolerogenic default, endogenous DCs have lost IRF8 and therefore cannot express IDO—but they also cannot express IL-12, rendering them functionally inert, able to neither instruct immunity nor regulate it. The alpha-DC1, with restored IRF8, possesses the molecular capacity for IDO expression, but its perforin-dependent elimination within days prevents the sustained IFN-γ exposure required to trigger the kynurenine/AhR autocrine maintenance loop [93,94]. Three brakes are therefore hierarchically organized: the temporal brake (perforin-dependent elimination constraining IFN-γ to days rather than the 2–7 day IDO installation window), the bimodal iNOS brake (supraphysiological IL-12 driving NO above the IDO-destroying threshold), and the IRF8-IDO dependency brake (ensuring that only IRF8-competent cells possess IDO capacity while the tolerogenic default's IRF8-silenced cells cannot install IDO even under sustained IFN-γ). The pulsatile architecture exploits the same transcription factor dependency that creates the tolerogenic default: IRF8 is the master switch for both the instructional program the alpha-DC1 restores and the self-regulatory program that could theoretically undermine it, but the temporal code ensures the instructional program completes before the regulatory program engages.

4. The Correction Cascade

4.1. Four Temporal Phases

The alpha-DC1 initiates a self-amplifying cascade through four phases (Figure 2). **Phase 1 (hours):** The alpha-DC1 samples the local antigenic landscape through its retained uptake machinery, then migrates to draining lymph nodes via CCR7 and delivers supraphysiological IL-12p70. IL-12 upregulates IRF8 in NK and T cells through direct STAT4 signaling promoting epigenetic remodeling of the Irf8 locus [79,84], in parallel with indirect IL-12→IFN-γ→STAT1→IRF8 induction—two

© 2026 by the author(s). Distributed under a Creative Commons CC BY license.

Preprints.org (www.preprints.org) | NOT PEER-REVIEWED | Posted: 15 April 2026 doi:10.20944/preprints202604.0868.v2

simultaneous pathways providing perturbation strength to overcome bistable hysteresis. This handoff is specific to monocyte-derived DC vaccines; Ferris showed cDC1 vaccines can drive tumor rejection through direct presentation independently of host cDC1 [59]. Antigen and instructional polarity transfer to endogenous lymph node-resident cDC1s through synaptic vesicle transfer and CD40L-induced tunneling nanotubes exclusive to type 1-programmed DCs [45,57]. The patient's disease determines the antigen curriculum: neoantigens, senescent cell debris, viral peptides, or mycobacterial components depending on what is present at the injection site. Nothing is preselected. Nothing is missed.

Figure 2. Alpha-DC1 Correction Cascade: Four Temporal Phases

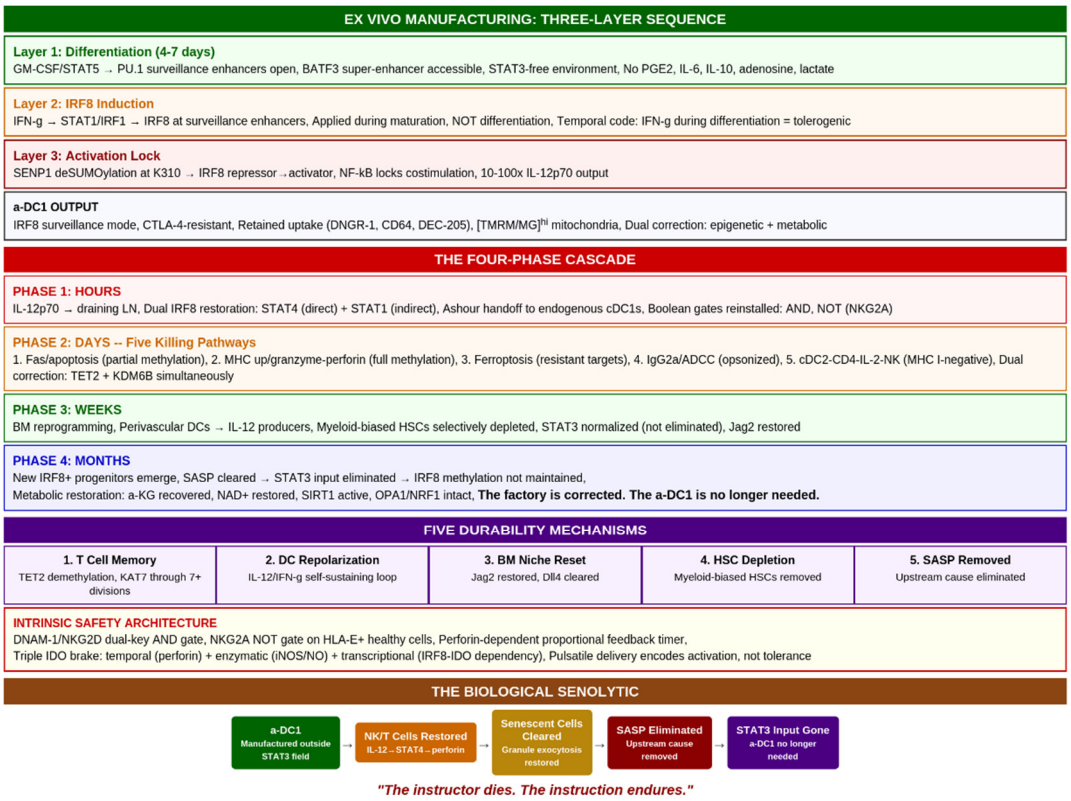

Figure 2. The alpha-DC1 correction cascade: four temporal phases. The alpha-DC1, manufactured ex vivo outside the STAT3 field through a three-layer chromatin programming sequence, initiates a four-phase cascade: IL-12 delivery with dual STAT4/STAT1 IRF8 restoration and endogenous DC handoff (Phase 1, hours); systemic IFN-γ-mediated target killing through five parallel pathways calibrated to target methylation state, opsonization status, and MHC I expression—with the balance between pathways dynamically responsive to target state changes, such as radiation-induced MHC-I upregulation that shifts vulnerability from NK-mediated missing-self killing to CTL-mediated antigen recognition, with doubly convergent correction removing both DNA methylation (TET2) and H3K27me3 (KDM6B/JMJD3) simultaneously (Phase 2, days); bone marrow niche reprogramming with selective myeloid-biased HSC depletion and Notch Jag2 normalization (Phase 3, weeks); and emergence of IRF8-competent progenitors with restored metabolic fitness following SASP clearance (Phase 4, months). Five durability mechanisms maintain the corrected state. Intrinsic safety is encoded in DNAM-1/NKG2D dual-key selectivity, NKG2A brake on healthy cells, and perforin-dependent elimination ensuring pulsatile delivery. The biological senolytic principle is illustrated: the alpha-DC1 restores immune-mediated senescent cell clearance, removing the upstream cause of its own necessity.

Phase 2 (days): Educated T cells with epigenetically stabilized IFN-γ traffic systemically. IFN-γ acts on every cell type encountered: on maturing DCs, it locks IL-12 competence; on MDSCs, it kills through Bcl2a1 repression and forces survivors to differentiate into antigen-presenting cells; on the chemokine landscape, it suppresses the Treg-recruiting CCL22 while maintaining effector-recruiting

© 2026 by the author(s). Distributed under a Creative Commons CC BY license.

Preprints.org (www.preprints.org) | NOT PEER-REVIEWED | Posted: 15 April 2026 doi:10.20944/preprints202604.0868.v2

CXCL9 and CXCL10, reversing immune cell trafficking from suppressor-dominant to effector-dominant; on Tregs, IL-12 converts them to IFN-γ-producing effectors. On target cells with partial IRF8 methylation, IFN-γ restores Fas sensitivity, BCL-2 repression, FLIP downregulation, and Bax activation through all five apoptotic pathways. On targets with full IRF8 methylation, IFN-γ demethylates antigen-presenting machinery (TAP-1/2, LMP-2/7) through IRF1 (which remains IFN-γ-responsive even when IRF8 is silenced [127]) for granzyme/perforin killing. Targets resistant to both pathways undergo ferroptosis through system xc^- suppression [58], including direct CD8+ T cell contact-dependent GPX4 downregulation [126,128]. A fourth killing mechanism operates through antibody-dependent cellular cytotoxicity: IL-12/IFN-γ drives IgG2a class-switching [87], and macrophages—required for IL-12-mediated tumor rejection—kill opsonized targets through FcγRII/III engagement [205]. A fifth mechanism addresses MHC I-negative targets resistant to CD8 T cell recognition: IL-12-mediated Treg conversion functionally depletes intratumoral Tregs, unleashing a cDC2-dependent pathway in which conventional CD4 T cells produce IL-2 that activates NK cell-mediated killing of MHC I-deficient tumors—as Zhang and colleagues demonstrated in Science Immunology (2026), where selective intratumoral Treg ablation controlled CD8 T cell-resistant cancers through this cDC2–CD4–IL-2–NK axis [214]. The correction is doubly convergent: TET2 removes DNA methylation while IFN-γ-induced KDM6B/JMJD3 removes H3K27me3 [192,193]. Mikulski demonstrated in Nature Structural and Molecular Biology (2025) that H3K27me3 depletion persists through cell divisions, providing heritable transcriptional memory [194]. Cells surviving all killing mechanisms undergo passive IRF8 demethylation over subsequent divisions as DNMT activity ceases following SASP removal, through replication-dependent dilution of oxidized methylcytosines [129].

Phase 3 (weeks): Educated T cells reach the bone marrow perivascular niche. IFN-γ reprograms perivascular DCs from IL-1β to IL-12 producers and selectively differentiates myeloid-biased HSCs through terminal differentiation while sparing balanced HSCs, which express lower IFN-γ receptor levels [46,121]. A critical distinction: the cascade normalizes rather than eliminates STAT3; STAT3 is required for HSC survival, and STAT3-deficient HSPCs show mitochondrial dysfunction and rapid aging [122,123]. Reducing STAT3 to physiological levels restores normal hematopoiesis [124], and STAT5, not STAT3, is the primary driver of HSC self-renewal [125]. The cascade also addresses the niche-level lock: Matteini showed aging sinusoidal endothelial cells lose Jagged-2, triggering Notch cis-inhibition locking myeloid expansion [142]—SASP clearance restores sinusoidal function while IFN-γ eliminates cis-inhibited cells.

Phase 4 (months): New myeloid progenitors emerge with IRF8 expressed because the STAT3-C/EBPβ emergency signal has been dismantled. The factory that was producing tolerogenic DCs and MDSCs now produces functional immune cells. Soyano demonstrated intratumoral DC1 delivery reduced bone marrow metastasis-initiating cells, with DC1-primed Th1 cells migrating to marrow in an IFN-γ-dependent manner [139].

© 2026 by the author(s). Distributed under a Creative Commons CC BY license.

Preprints.org (www.preprints.org) | NOT PEER-REVIEWED | Posted: 15 April 2026 doi:10.20944/preprints202604.0868.v2

4.2. Resolution, Durability, and Epigenetic Persistence

The correction persists because the cascade removes the upstream cause, not merely the downstream consequence. Licensed effectors clear senescent cells; SASP removal eliminates IL-6 driving STAT3; without STAT3, DNMTs are not induced; without DNMT activity, IRF8 methylation is not maintained through cell divisions; new progenitors emerge with IRF8 expressed; the IL-12/IFN-γ feedback loop becomes self-sustaining. The alpha-DC1 is no longer needed.

Five durability mechanisms operate simultaneously: T cell epigenetic memory through TET2-mediated IFN-γ locus demethylation maintained by KAT7 through seven divisions [18,85]; endogenous DC repolarization through the self-sustaining IL-12/IFN-γ loop; bone marrow niche reprogramming with perivascular DCs converted to IL-12 producers; selective myeloid-biased HSC depletion while balanced HSCs repopulate [46]; and SASP source removal eliminating the upstream signal. The alpha-DC1 is eliminated within days primarily through perforin-dependent killing by the effectors it educated [96], ensuring pulsatile rather than chronic cytokine delivery. Daman demonstrated that BCG colonizes bone marrow, reprograms HSPCs, drives T cell-dependent anti-tumor responses, and synergizes with checkpoint blockade [140]—establishing that single immunotherapy interventions can durably reprogram the HSPC compartment.

The epigenetic architecture ensures these marks persist. Wilson recognized in 2005 that DNA methylation encodes T cell lineage commitment through stable, heritable chromatin states [15]. The alpha-DC1's IFN-γ cascade activates STAT1, which recruits CBP to deposit H3K27ac at the same loci STAT3 had silenced [16], and STAT3-dependent NFIL3 repression at the IL-12b distal enhancer [53] is reversed—the same enzymatic machinery writing opposite programs depending on which transcription factor recruits it. Ostuni demonstrated in 2013 that IFN-γ creates latent enhancers with persistent H3K4me1 serving as epigenomic memory [17]. Mikulski proved H3K14ac and H4K16ac are maintained through at least seven divisions by KAT7 without ongoing transcription [18]. Cowley demonstrated in Science (2026) that CpG-rich regions retain modifications for the organism's lifespan through a self-reinforcing circuit of DNA demethylation, methylation-sensitive transcription factor recruitment, and H2A.Z incorporation [19]. The genomic locations where the alpha-DC1's IFN-γ cascade writes its corrective marks were selected by evolution to retain modifications across cell divisions. The instructor dies. The instruction endures.

5. Platform Architecture and Clinical Evidence

The DCVax-Direct platform manufactures the alpha-DC1 on the EDEN closed-system bioreactor. Phase I: 149 intratumoral injections across 40 patients, no dose-limiting toxicities, with IL-12p40 secretion significantly associated with survival (P = 0.024) [20]. DCVax-L Phase III in glioblastoma: median OS 19.3 months, 13% surviving beyond 5 years in the most immunosuppressive solid tumor microenvironment [21]. Safety across >1,000 vaccinees with no treatment-related autoimmune events reflects correct bidirectional gate installation—NKG2A brake on healthy cells, perforin-dependent elimination ensuring pulsatile delivery, and the p53/MDM2 threshold ensuring each cell's response matches its functional context. A critical distinction from systemic recombinant IL-12 (which caused lethal toxicity when priming dose was omitted [131]) must be noted: the alpha-DC1 delivers IL-12 locally at the injection site and draining lymph node, pulsatilely through perforin-dependent elimination, and self-limitingly through the proportional feedback timer in which more effectors accelerate DC clearance. The DCVax-Direct Phase I safety profile confirms this distinction empirically. The alpha-DC1 also carries BCG-derived PAMPs that activate TLR2/TLR4/TLR9 in every endogenous DC contacted during the instructional handoff, converting a single injection into a maturation relay propagating through the endogenous DC network [45].

© 2026 by the author(s). Distributed under a Creative Commons CC BY license.

Preprints.org (www.preprints.org) | NOT PEER-REVIEWED | Posted: 15 April 2026 doi:10.20944/preprints202604.0868.v2

6. Discussion

6.1. Summary of the Framework

The evidence reviewed here establishes that the tolerogenic default is not a collection of independent failures but a single epigenetic state installed by one convergent molecular chain: SASP cytokines activate STAT3, STAT3 recruits DNMTs and EZH2 to silence IRF8, and IRF8 silencing collapses the immune surveillance network while armoring target cells against killing. Each link has been independently demonstrated in non-malignant myeloid cells or aged hematopoietic progenitors: aged mesenchymal SASP activates STAT3 in co-cultured HSPCs (Gnani 2019), IL-6 from the aging niche drives the DNMT axis (Zioni 2023), IL-10/STAT3 epigenetically silences IRF transcription factors in primary human monocytes (Mishra 2025), and IRF8 declines with aging as the sole gene with conserved decreases across human and murine HSPCs [86]. The single experiment connecting these links in sequence—SASP exposure through STAT3 phosphorylation through DNMT induction through IRF8 bisulfite sequencing in sorted aged HSPCs—has not been published, but the convergent evidence from multiple independent systems constitutes a level of proof that exceeds hypothesis. Each phase transition of the correction cascade is independently demonstrated: IFN-γ directly upregulates IRF8 while suppressing STAT3 in bone marrow myeloid progenitors (de Bruin 2012; Waight, ref [197]), DNMT inhibition restores IRF8 and corrects bilateral disarmament simultaneously in vivo (Mattei, ref [101]), and IL-12 drives TET2-mediated demethylation enabling heritable epigenetic reprogramming (Zebley, ref [85]). The STAT3-DNMT-IRF8 axis is the only identified mechanism that simultaneously explains dysfunction across antigen presentation, effector differentiation, apoptotic resistance, genome surveillance, and pathogen killing from a single epigenetic event.

6.2. Limitations

Several limitations warrant consideration. The bilateral disarmament model is now substantially supported in single systems: Greeneltch showed IRF8 silencing simultaneously reduced Fas-mediated apoptosis and accelerated tumor growth through escape from IFN-γ/FasL-dependent immune killing, with the growth advantage disappearing in IFN-γ-deficient hosts [99]; Hu showed IRF8 loss in MDSCs conferred resistance to CTL killing through decreased Bax and increased Bcl-xL [100]; Mattei showed 5-azacitidine restored both immune infiltration and IRF8 expression simultaneously in IRF8-deficient mice [101]; Montoya showed IRF8 delivery to both tumor and myeloid cells was required for survival benefit in glioblastoma, with IRF8 restoring tumor suppressor function while reprogramming MDSCs into antigen-presenting cDC1s [102]; Yang established IRF8 promoter methylation as the molecular determinant of both apoptotic resistance and metastatic phenotype [103]; and Wang demonstrated a bifunctional CpG-STAT3 decoy simultaneously upregulated IRF8, downregulated DNMTs, and activated anti-leukemic immunity—reversing bilateral disarmament from one intervention targeting the shared signaling node [138]. Additionally, Zhu demonstrated that autocrine IL-6 activates the STAT3-DNMT axis in MDSCs, producing IRF8 promoter hypermethylation that disables the identical apoptotic effectors—caspase-3, BCL-2, Bcl-xL, Bax, and Fas—that Yang showed are dysregulated by IRF8 methylation in the tumor compartment [103,120]. The immune-side study names the target-side effectors. Three independent intervention classes—epigenetic (5-azacitidine restoring IRF8), signaling (STAT3 decoy reversing bilateral disarmament), and instructional (alpha-DC1 restoring IL-12)—each reverse distinct components of the same axis, collectively demonstrating that targeting this shared architecture produces system-level correction.

The STAT3-IRF8 chain operates in non-malignant systems: Waight showed SASP cytokines facilitated STAT3-dependent IRF8 downregulation in normal bone marrow progenitors [197]; Harroch showed IL-6 directly downregulates IRF8 in myeloid cells [198]; Kim confirmed IL-6 activates STAT3 and increases DNMT1 in healthy hematopoietic cells [177]. Molony found no age-related CpG methylation difference at IRF8 in mature monocytes, attributing IRF8 decline to

© 2026 by the author(s). Distributed under a Creative Commons CC BY license.

Preprints.org (www.preprints.org) | NOT PEER-REVIEWED | Posted: 15 April 2026 doi:10.20944/preprints202604.0868.v2

impaired IFNAR-to-IRF8 induction [55]. This refines rather than contradicts the framework: the methylation event operates at the progenitor stage [33], while mature monocytes may maintain suppression through additional mechanisms. The measurement must target sorted progenitors.

Direct interrogation of the Adelman datasets from young versus aged human HSCs [189] reveals age-associated epigenetic changes at the IRF8 locus. Formal differential peak analysis (Table S3, GEO: GSE104404) identifies one statistically significant change: H3K27ac at an IRF8 enhancer (chr16:85,936,593–85,936,978) is decreased nearly twofold in aged HSCs (FC = −1.92, classified "Decreased"), indicating active enhancer inactivation. H3K4me3 at the IRF8 promoter trends downward 43% (FC = −1.43) but does not reach significance. H3K27me3 peaks show mixed directions without significance. DNA methylation (ERRBS, GEO: GSE104405) is low in most donors but one aged donor shows focal CpG hypermethylation at the core IRF8 promoter CpG island. This pattern—significant enhancer H3K27ac loss preceding promoter methylation—is precisely what the enhancer cascade model predicts, corroborated by comprehensive HSC epigenomic profiling [187,188,190,191].

Patel demonstrated that basal STAT3 protects HSC function [171]; the framework specifically implicates sustained STAT3 hyperactivation, not STAT3 presence, consistent with the temporal code principle [105]. Zhivaki found DC migration, not cytokine production, may be rate-limiting in aging [40]; the alpha-DC1 retains CCR7-mediated migratory capacity.

Three additional limitations merit note. First, IRF8 is a GWAS susceptibility factor for autoimmune diseases including multiple sclerosis and systemic lupus erythematosus, and IRF8-deficient mice are resistant to experimental autoimmune encephalomyelitis [132]. While the alpha-DC1 does not systemically overexpress IRF8 but restores the IL-12/IFN-γ axis inducing IRF8 in a context-dependent manner, and the DCVax safety profile confirms no autoimmune events, patients with active autoimmune conditions require caution. Second, the cascade acts primarily on newly primed T cells, not reversing TOX-driven epigenetic exhaustion in existing TILs [133]. IL-12 preconditioning prevents exhaustion in naïve T cells by reducing PD-1, LAG-3, and TOX expression [134], and IL-12-STAT4 signaling is redirected by prior antigen-receptor signals to promote memory rather than terminal exhaustion [135]. The Zhivaki finding that CD4+ T cells eradicated tumors in aged mice suggests the cascade bypasses the exhausted CD8+ compartment by engaging cytolytic CD4+ effectors [40]. Third, CHIP clones with DNMT3A mutations retain intrinsic competitive advantage independent of SASP [136], and while anti-inflammatory interventions can attenuate TET2-driven clonal expansion [137], DNMT3A clones may persist; patients with high-VAF CHIP may require combination approaches. Additionally, the four-phase cascade model, while consistent with published data on each individual phase, has not been demonstrated as a connected sequence in a single in vivo system. However, every individual phase transition is supported by independent mechanistic evidence already cited in this manuscript, making the connected experiment a confirmatory rather than discovery-level priority.

6.3. Relationship to Existing Paradigms

The framework is distinct from but compatible with existing paradigms. The mregDC program identified as a conserved regulatory DC state may represent the terminal output of STAT3-driven IRF8 suppression—not a distinct DC lineage but the functional consequence of the tolerogenic default described here. This interpretation is testable by IRF8 ChIP-seq in sorted mregDCs versus immunogenic cDC1s from the same tumor. Trained immunity acts on already-formed myeloid cells through H3K4me3 and H3K27ac modifications at innate immune gene promoters without addressing IRF8 promoter methylation as an upstream failure mechanism; the alpha-DC1 restores instructional capacity by manufacturing cells outside the suppressive field, addressing a different hierarchical level. The approaches are complementary. Alternative models—T cell metabolic insufficiency, mitochondrial effector dysfunction, thymic involution—describe real effector compartment phenomena but cannot explain simultaneous multi-compartment collapse. T cell exhaustion is a consequence of failed DC instruction: Zhivaki demonstrated DC correction eradicated tumors where checkpoint blockade targeting exhausted T cells failed entirely [40].

© 2026 by the author(s). Distributed under a Creative Commons CC BY license.

Preprints.org (www.preprints.org) | NOT PEER-REVIEWED | Posted: 15 April 2026 doi:10.20944/preprints202604.0868.v2

You and colleagues' mitochondrial fitness findings provide independent validation: intratumoral injection of [TMRM/MG]^{hi} cDC1s triggered strong antitumor immunity [143], and Molina and Haldar confirmed OPA1-NRF1 operates specifically in cDC1s, not cDC2s [144]—consistent with cDC1-specific vulnerability to STAT3-driven silencing. This model explains the upstream cause You and colleagues left unresolved: the alpha-DC1 is inherently a [TMRM/MG]^{hi} cell because it differentiates outside the SASP-STAT3 metabolic stress field. Friedrich demonstrated in Nature (2025) that mRNA delivery of DLL1/FLT3L/IL-7 expanded lymphoid progenitors and restored DC function in aged mice [172]—addressing niche factor deficit but not IRF8 methylation already installed. Ross showed in Nature (2024) that depleting myeloid-biased HSCs restored balanced hematopoiesis [173]—consistent with progenitor-level failure but requiring repeated depletion because the SASP niche remains intact. The alpha-DC1 addresses the niche through Phase 3 reprogramming and Phase 4 SASP clearance.

The EZH2 inhibitor paradox validates the dual-mark mechanism: GSK126 paradoxically expanded MDSCs and suppressed immunity despite effective tumor killing in immunodeficient mice [184]; Qiang replicated this with UNC1999 [185]. The framework explains directly: EZH2 inhibition removes H3K27me3 but not DNA methylation, releasing progenitors into a landscape where IRF8 is still absent, defaulting to MDSC expansion—removing one lock without removing the other makes things worse. This generates a testable prediction: alpha-DC1 + EZH2 inhibitor should synergize through simultaneous dual-mark removal. Chibaya demonstrated the principle in Nature Cancer: EZH2 inhibition remodeled the SASP to enhance immune surveillance, but only with immune activation [186]. Senolytic approaches show analogous limitations: Luo showed dasatinib + quercetin promoted tumor progression [170]; Gadecka showed non-specific bidirectional chromatin changes rather than clean reversal [174]. Senolytics cannot reverse DNMT-mediated IRF8 methylation already installed in myeloid progenitors, because the epigenetic damage persists independently of whether the SASP source is cleared. The IFN-γ cascade also generates a predictable adaptive resistance: IFN-γ upregulates CD47 on surviving target cells through JAK1/STAT1/IRF1, increasing SIRPα-mediated phagocytic resistance [201], and cancer cells under cognate T cell attack dynamically enhance CD47 surface expression independently of the myeloid CD47-SIRPα axis [202]. This creates a testable combination prediction: alpha-DC1 combined with CD47/SIRPα blockade should synergize, because CD47 blockade preferentially enhances cGAS-STING-dependent DNA sensing in DCs rather than macrophages by enabling NOX2-dependent phagosomal alkalinization preserving tumor mitochondrial DNA [203], and the alpha-DC1's restored IRF8 provides the STING scaffolding protein required for this signal transduction [104]. The framework thus predicts that anti-CD47 therapy would show preferential efficacy in patients receiving alpha-DC1 vaccination.

A critical nuance: STAT3 is essential for normal immunity (germline LOF causes hyper-IgE syndrome). The framework implicates sustained activation specifically.

Metformin provides compelling pharmacological validation of the SASP→STAT3→DNMT→IRF8 framework. Metformin attenuates three of four nodes in the chain: it suppresses the SASP at the mesenchymal source, with Petrocelli demonstrating reduced senescence markers and SASP in human fibro-adipogenic progenitors [220]; it inhibits STAT3 phosphorylation through AMPK-dependent and AMPK-independent mechanisms in myeloid cells [221]; and it suppresses NF-κB-driven IL-6 transcription feeding the STAT3 axis. But metformin cannot reverse DNMT-mediated IRF8 methylation already installed. This explains every paradox in the metformin-aging literature: the ~31% cancer incidence reduction (the fraction of cancers emerging in the window metformin extends before the IRF8 threshold is crossed), the mortality benefit in diabetics below non-diabetics (metformin suppresses the accelerated SASP-like environment of chronic hyperinsulinemia more effectively than endogenous homeostasis), and the failure to extend lifespan in the NIA Interventions Testing Program (by the time aged mice are tested, many progenitors have already crossed the irreversible threshold) [222]. The TAME trial—the first RCT designed to test whether a single agent can slow age-related multimorbidity—is essentially testing the upstream half of this mechanism chain.

© 2026 by the author(s). Distributed under a Creative Commons CC BY license.

Preprints.org (www.preprints.org) | NOT PEER-REVIEWED | Posted: 15 April 2026 doi:10.20944/preprints202604.0868.v2

This architecture further predicts a paradox that has been experimentally confirmed: metformin suppresses STAT3 systemically but simultaneously inhibits the glycolytic switch that TLR-stimulated DCs require for IL-12 biosynthesis (Lock 5), producing tolerogenic rather than immunogenic DCs. Liu and colleagues demonstrated this directly—metformin-treated DCs showed reduced MHC-II, reduced costimulatory molecules, increased IL-10 and PD-L1, and enhanced Treg differentiation [223]. This model is the only one that predicts this outcome: hitting STAT3 is necessary but insufficient because IL-12 production requires the very metabolic program that metformin inhibits. Metformin slows the approach to the cliff edge but cannot rescue anyone who has already gone over. Only the alpha-DC1—manufactured outside the STAT3 field with its metabolic program intact—bypasses this paradox entirely. The epidemiological parallel extends to coffee polyphenols: caffeic acid and chlorogenic acid directly inhibit DNMT1 at low micromolar concentrations (IC50 0.9–2.3 μM), and habitual coffee consumption is associated with reduced cancer incidence across multiple cohort studies [224]—consistent with partial attenuation of DNMT-mediated methylation in individuals who have not yet crossed the bistable threshold. Braun demonstrated that IL-6 and IL-10 activate identical STAT3 yet produce opposing transcriptional programs—the difference encoded entirely in signal duration: artificially truncating STAT3 activation after IL-10 stimulation caused IL-10 to elicit an IL-6-like pro-inflammatory response [105]. The immune system reads STAT3 signal duration, not cytokine identity. The SASP corrupts this temporal code by converting transient STAT3 activation (which resolves through SOCS3 feedback within hours) into sustained activation (because the paracrine source never resolves), and it is sustained activation specifically that induces DNMT1 and drives IRF8 promoter methylation. Qing and Stark showed STAT1 and STAT3 compete for the same receptor phosphotyrosine motifs, with relative abundance determining cellular response [106]. The alpha-DC1's IL-12/IFN-γ cascade shifts this balance toward STAT1/STAT4 dominance, and its perforin-dependent elimination within days ensures the counter-signal is delivered in a pulsatile temporal pattern that encodes immune activation rather than tolerance. The pulsatile delivery is therefore not merely a safety feature—it is the mechanism by which the correct temporal code is written into the endogenous immune network. The temporal code applies to IL-12 itself, not only to STAT3. When IRF8-deficient myeloid cells produce chronic, unresolved IL-12—as occurs in neurodegeneration, where microglia that have lost IRF8-dependent homeostatic identity default to sustained inflammatory output—the same cytokine that restores immunity becomes pathological: genetic ablation of IL-12 p40 or p35 reduced cerebral amyloid load and cognitive decline in Alzheimer's models [211], and IL-12 receptor deletion in neuroectodermal cells ameliorated pathology by restoring oligodendrocyte homeostasis and microglial phagocytosis [212]. The alpha-DC1's perforin-dependent elimination prevents IL-12 from becoming the sustained, destructive signal that the tolerogenic default's dysfunctional myeloid cells produce. Pulsatile IL-12 from a correctly manufactured DC writes activation. Chronic IL-12 from a broken one writes destruction. The signal is identical. The temporal code is everything.

6.4. Testable Predictions

The framework generates specific testable predictions (Table 1). First, STAT3 activation in myeloid progenitors cultured with SASP cytokines should induce DNMT1/3B, methylate IRF8, and produce cells incapable of IL-12; culture in STAT3-free conditions should prevent this. This experiment is achievable within a standard laboratory timeframe. Second, IRF8 promoter methylation in CD14+ monocytes should correlate with immune competence across aging, cancer, and chronic infection cohorts—a translational study performing bisulfite sequencing and ATAC-seq on monocytes from healthy adults, cancer patients, aging individuals, and CHIP carriers would test whether IRF8 chromatin state predicts outcomes including vaccine response, cancer recurrence, and infection susceptibility. Third, the four-phase cascade predicts specific sequential molecular events: IL-12p70 delivery and endogenous DC handoff (hours), systemic IFN-γ with MDSC depletion and Treg conversion (days), bone marrow perivascular DC reprogramming (weeks), and emergence of IRF8-competent progenitors (months). Each transition is measurable and each must occur for the

© 2026 by the author(s). Distributed under a Creative Commons CC BY license.

Preprints.org (www.preprints.org) | NOT PEER-REVIEWED | Posted: 15 April 2026 doi:10.20944/preprints202604.0868.v2

model to hold. Fourth, STING pathway agonists should show preferential efficacy in patients with preserved IRF8, because IRF8 scaffolds STING polymerization through a transcription-independent role [104]—if IRF8 is silenced, STING agonists would fail regardless of dose because the scaffolding protein is absent. IRF8 methylation status could serve as a companion diagnostic. Fifth, periodic alpha-DC1 administration calibrated to IRF8 methylation status could restore immune competence before epigenetic silencing deepens beyond reversibility—a shift from treating disease after organ-level manifestation to correcting the upstream instructional deficit. Basrai demonstrated that DNA methylation instability at epigenetically stable loci correlates with cardiovascular risk and reduced survival through maladaptive clonal expansion [91], corroborating IRF8 methylation as a biomarker for the phase transition. Sixth, the triple IDO brake predicts that serum kynurenine/tryptophan ratio should decline following alpha-DC1 vaccination—in direct contrast to the increases observed with checkpoint blockade, where Li and colleagues showed nivolumab caused a 37% K/T increase at week 4 with patients whose ratio rose more than 50% showing significantly worse survival [213]. The bimodal NO mechanism predicts an inverse correlation between rising serum nitrite/nitrate (confirming iNOS activation) and declining K/T ratio (confirming IDO suppression)—a pattern never yet documented in any immunotherapy trial and directly testable with existing validated assays. Seventh, IRF8 chromatin state defines three clinically distinguishable states measurable in circulating CD14+ monocytes: State 1 (IRF8-absent: promoter methylation >60%, no IL-12p70 upon TLR stimulation), State 2 (IRF8-surveillance: methylation <20%, IL-12p70 >100 pg/mL upon stimulation), and State 3 (IRF8-proliferative: unmethylated but engaged at proliferative rather than surveillance enhancers, no IL-12p70 despite IRF8 protein present). State 1 is distinguishable by bisulfite sequencing; States 2 and 3 require ex vivo DC differentiation with functional IL-12p70 assay. Phosphorylated STAT3 in circulating CD14+ monocytes, measurable by phospho-flow cytometry, directly quantifies the STAT3 hub driving the tolerogenic default and predicts the transition between states. Eighth, the combination of IRF8 methylation, K/T ratio, and IL-12p70 predicts three distinct immunotherapy failure modes that no individual biomarker can distinguish: epigenetic incompetence (IRF8 methylated, patient cannot produce IL-12 regardless of therapy), metabolic suppression (IRF8 unmethylated but elevated K/T ratio suppresses IL-12 output through the kynurenine/AhR axis), and adaptive resistance (initially responsive but K/T ratio rises over treatment cycles as the IDO feedback loop installs). SOCS3 promoter methylation in CD14+ monocytes, which reaches 60% in AML marrow versus zero in remission [114,115], provides a direct readout of Loop 1 engagement and predicts whether the STAT3 feed-forward circuit is locked. Ninth, systemic COX-2 inhibition before alpha-DC1 administration should synergize by reducing PGE2 concentration in the tumor microenvironment, protecting endogenous DCs from the PGE2 chromatin trap during Phase 2 repolarization while the alpha-DC1 itself is unaffected (manufactured ex vivo). Li and colleagues demonstrated in 1,748 NSCLC patients that NSAID use was independently associated with improved progression-free survival (HR 0.72, p=0.005) and overall survival (HR 0.76, p=0.04) when combined with checkpoint inhibitors, with aspirin specifically lowering serum PGE2 [244]. Punyawatthananukool confirmed in Nature Communications that PGE2-EP2/EP4 signaling impairs bioenergetics and ribosome biogenesis across all tumor-infiltrating immune cells [245]—meaning PGE2 reduction benefits not just DCs but every immune cell the cascade is restoring. The Bayerl finding that PGE2-induced cDC1 dysfunction depends on IRF8 loss [242] means COX-2 inhibition and the alpha-DC1 cascade address the same molecular target from opposite directions: COX-2 inhibition prevents new IRF8 loss in endogenous DCs, while the cascade restores IRF8 in cells that have already lost it. Tenth, the α-ketoglutarate/succinate ratio in circulating CD14+ monocytes should rise as the cascade breaks Loop 2: mitochondrial restoration in Phase 4 recovers α-KG production while eliminating the succinate and fumarate accumulation that competitively inhibits TET-mediated demethylation at the IRF8 locus [148,149]. This ratio is measurable by targeted metabolomics and directly predicts TET2 reprogramming capacity in myeloid cells [149]. Eleventh, whole blood NAD+ should recover from the depleted levels characteristic of aged and chronically inflamed states as Loop 3 is broken: SASP clearance restores de novo NAD+ biosynthesis [217], reactivating SIRT1-mediated

© 2026 by the author(s). Distributed under a Creative Commons CC BY license.

Preprints.org (www.preprints.org) | NOT PEER-REVIEWED | Posted: 15 April 2026 doi:10.20944/preprints202604.0868.v2

STAT3 deacetylation [151,152]. Validated enzymatic cycling assays now enable clinical-grade NAD+ measurement from small blood volumes [246]. Twelfth, H3K27me3 at the IRF8 locus should decline as the dual-mark silencing described in Section 2 is reversed: TET2 removes DNA methylation while KDM6B/JMJD3 removes the Polycomb mark simultaneously [192,193]. Low-input chromatin profiling methods have been applied to peripheral blood monocytes profiling H3K27me3 in clinical populations [247], making locus-specific measurement at IRF8 technically feasible and providing direct confirmation of whether the EZH2 component of dual-mark silencing has been reversed. Thirteenth, if the cascade truly corrects the upstream cause of immune aging, epigenetic clock measures—particularly DunedinPACE (rate of aging) and GrimAge2 (mortality prediction)—should decelerate or reverse following treatment. Fahy and colleagues demonstrated a 2.5-year mean epigenetic age reversal with immune reconstitution in the TRIIM trial [248], and single-cell immune aging clocks have revealed that BCG vaccination can rejuvenate CD8+ T cell epigenetic age in a subset of recipients [249]. No cancer immunotherapy trial has measured epigenetic clock changes—this would be the first demonstration that correcting DC instruction reverses systemic biological aging. Fourteenth, anti-dsDNA antibodies and ANA titers should remain stable or decline following alpha-DC1 vaccination, confirming that the restored IRF8 axis reinstalls B cell anergy checkpoints rather than breaching them. Pathak demonstrated that IRF8-deficient mice spontaneously produce anti-dsDNA antibodies [36]; the prediction is that IRF8 restoration corrects this deficit. This is consistent with the genetics: the SLE risk allele rs2280381 decreases IRF8 expression in monocytes through reduced PU.1 binding, and the pathogenic DN2 B cells expanded in active lupus are characterized by low IRF8—confirming that IRF8 loss, not gain, breaches tolerance checkpoints. No DC vaccine trial—including DCVax-L [21] and sipuleucel-T [250]—has published systematic autoantibody monitoring data, despite IRF8's established GWAS associations with autoimmune diseases. Additionally, CD47 expression on tumor cells should be monitored as an adaptive resistance biomarker: IFN-γ upregulates CD47 through JAK1/STAT1/IRF1 signaling, and cancer cells under immune attack dynamically acquire CD47-mediated resistance independently of the myeloid axis [201,202]. Rising CD47 would signal the need for anti-CD47 combination therapy, for which the alpha-DC1's restored IRF8 provides the STING scaffolding required for cGAS-dependent phagocytic sensing [104,203].

Table 1. Testable predictions and biomarker panel for the alpha-DC1 correction cascade. Fourteen predictions are listed with corresponding biomarkers, validated assay platforms, expected trajectories following alpha-DC1 vaccination versus checkpoint blockade comparators, and specific falsification criteria. A fifteenth prediction (COX-2/PGE2 combination) is described in the text. Six additional biomarkers measure feedback loop engagement (α-KG/succinate for Loop 2, NAD+ for Loop 3), dual-mark reversal (H3K27me3 at IRF8), systemic epigenetic rejuvenation (DunedinPACE), autoimmune safety (anti-dsDNA/ANA), and adaptive resistance emergence (CD47/sSIRPα). The serum kynurenine/tryptophan ratio and serum nitrite/nitrate represent the primary pharmacodynamic readouts for confirming the bimodal NO threshold has been crossed and IDO enzymatic activity suppressed. IRF8 promoter methylation in CD14+ monocytes serves as the upstream companion diagnostic. Phosphorylated STAT3 in circulating monocytes directly quantifies the tolerogenic default hub. SOCS3 promoter methylation measures Loop 1 feed-forward engagement. The combination of IRF8 methylation, K/T ratio, and IL-12p70 distinguishes three failure modes (epigenetic incompetence, metabolic suppression, adaptive resistance) inaccessible to any individual biomarker.

Prediction	Biomarker	Assay	Expected (α-DC1)	Comparator (CPI)	Falsification
SASP–STAT3–IRF8 chain	IRF8 promoter CpG methylation (CD14+ monocytes)	Bisulfite-seq / ATAC-seq	Declining with each cycle	Not measured	Methylation unchanged after Phase 4

© 2026 by the author(s). Distributed under a Creative Commons CC BY license.

Preprints.org (www.preprints.org) | NOT PEER-REVIEWED | Posted: 15 April 2026 doi:10.20944/preprints202604.0868.v2

IL-12 restoration	Serum IL-12p70	ELISA	Pulsatile spikes (hours post-injection)	Absent	No detectable IL-12p70
IDO suppression (bimodal NO)	Serum K/T ratio	LC-MS/MS	Declining from ~60–80 toward ~30–35 µmol/mmol	37% increase at wk 4 (Li 2019)	K/T rises or unchanged
iNOS threshold crossed	Serum NOx (nitrite/nitrate)	Griess assay	Rising above ~60 µM	Not measured	NOx unchanged from baseline
Inverse NO–IDO correlation	NOx↑ with K/T↓ (paired draws)	Paired Griess + LC-MS/MS	Inverse correlation	Never documented	No correlation
STING competence	IRF8 methylation as companion Dx	Bisulfite-seq	Predicts STING agonist response	Not available	IRF8-silenced respond equally
Senescent cell clearance	p16/p21; SASP (IL-6, GDF-15)	IHC / Luminex	Declining (Phase 3–4)	Not measured	SASP unchanged at 6 mo
STAT3 hub activation	pSTAT3 (Y705) in CD14+ monocytes	Phospho-flow cytometry	Declining toward baseline	Elevated; predicts CPI failure	pSTAT3 unchanged
Loop 1 engagement	SOCS3 promoter methylation (CD14+)	Bisulfite-seq	Declining (brake restored)	60% in AML vs 0% remission	SOCS3 methylation persists
Three failure modes	IRF8 meth + K/T + IL-12p70 combination	Composite panel	Distinguishes epigenetic / metabolic / adaptive	Not measured as combination	Combination not predictive
Mitochondrial restoration	Circulating cell-free mtDNA	qPCR / ddPCR	Declining (Phase 4)	Not measured	ccf-mtDNA unchanged
Metabolic fitness	PBMC mitochondrial respiration	Seahorse XF / Oroboros	OXPHOS capacity increasing	Not measured	Respiration unchanged
Loop 2 metabolic trap	α-KG/succinate ratio (CD14+ monocytes or plasma)	LC-MS/MS or colorimetric kit	Ratio rising toward 1.5–2.0 (Phase 4)	Not measured	Ratio unchanged or declining
Loop 3 acetylation lock	Whole blood NAD+	NADMED enzymatic cycling (CE-marked) or LC-MS/MS	Rising from ~20 toward ~33 µmol/L (Phase 4)	Not measured	NAD+ unchanged from baseline

© 2026 by the author(s). Distributed under a Creative Commons CC BY license.

Preprints.org (www.preprints.org) | NOT PEER-REVIEWED | Posted: 15 April 2026 doi:10.20944/preprints202604.0868.v2

Dual-mark reversal	H3K27me3 at IRF8 locus (CD14+ monocytes)	CUT&Tag-qPCR or CUT&RUN	H3K27me3 declining at IRF8 enhancer (Phase 2–4)	Not measured	H3K27me3 persists at IRF8
Systemic epigenetic reversal	Epigenetic age (DunedinPACE / GrimAge2)	CLIA-certified methylation array	Rate of aging decelerating; biological age decreasing	Not measured in immunotherapy	DunedinPACE unchanged or accelerating
Safety: autoimmune surveillance	Anti-dsDNA Ab; ANA titer	ELISA / IIF (HEp-2)	Stable or declining (anergy restored)	ANA rises in 15–25% of CPI patients	New anti-dsDNA or ANA ≥1:160 post-vaccination
Adaptive resistance	CD47 MFI on CTCs or sSIRPα	Flow cytometry (B6H12) / ELISA	Rising CD47 signals need for anti-CD47 combination	Not monitored	CD47 unchanged despite progression

6.5. Broader Implications

If validated, this framework would redefine the therapeutic target across oncology, infectious disease, and aging medicine from the effector compartment to the instructor. Current approaches—checkpoint blockade, adoptive cell transfer, recombinant cytokines, senolytics—operate downstream of the primary defect. Checkpoint blockade releases brakes on T cells that were never properly instructed. Adoptive cell transfer provides effectors without correcting the instruction that determines whether those effectors persist. Senolytics clear senescent cells without restoring the surveillance system that should prevent their reaccumulation. Each approach addresses a consequence while leaving the cause intact. The alpha-DC1 corrects the cause.

The implications extend beyond oncology. IRF8 promoter methylation as a predictive biomarker could identify individuals transitioning from immune competence to the tolerogenic default before disease manifests at the organ level—when cognition begins to decline, when latent infections reactivate, when vaccine responses wane. This represents a paradigm shift from reactive medicine (treating disease after organ-level manifestation) to preventive correction (restoring instructional capacity before the epigenetic silencing deepens beyond the window of reversibility). The Basrai finding that DNA methylation instability at stable loci predicts cardiovascular risk and survival [91] suggests this window is measurable and clinically actionable.

The cross-tissue parallel is striking. The STAT3→DNMT→epigenetic silencing chain operates identically in non-immune tissues: in fibroblasts, TGF-β induces DNMT3A-mediated SOCS3 methylation locking STAT3 activation and driving fibrosis across skin, lung, and kidney, reversible by restoring epigenetic control [107]. In bone, IRF8 silencing de-represses NFATc1 driving pathological osteoclastogenesis [108]. In microglia, IRF8 loss converts homeostatic sentinels to disease-associated phenotypes [76]. Mitochondrial dysfunction-associated senescence (MiDAS) directly links the metabolic collapse described in this framework to SASP production: damaged mitochondria release mtDNA into the cytosol, activating the cGAS-STING-IRF3 inflammatory pathway, while NAD+ depletion through increased CD38 activity induces a pseudohypoxic state disrupting nuclear-mitochondrial coordination [215]. The alpha-DC1 cascade addresses this by restoring mitochondrial quality through Phase 4 SASP clearance, predicting that circulating cell-free mtDNA should decline as mitochondrial integrity is restored. Each tissue has its own version of the same epigenetic trap. This model proposes that the STAT3-DNMT-IRF8 axis is sufficient to generate

© 2026 by the author(s). Distributed under a Creative Commons CC BY license.

Preprints.org (www.preprints.org) | NOT PEER-REVIEWED | Posted: 15 April 2026 doi:10.20944/preprints202604.0868.v2

the observed phenotype, while acknowledging that full causal validation across all domains requires prospective intervention studies. It does not exclude disease-specific modifiers but proposes that these operate on a shared upstream architecture defined by STAT3–IRF8 dynamics. But the immune system's version is upstream of all others—because the immune system is the quality control apparatus that should clear the senescent cells generating the SASP driving every downstream cascade. A Nature Medicine study of 18,701 participants across 34 countries demonstrated that cumulative physical and social exposome burden—including air pollution, socioeconomic inequality, and reduced green space access—accounted for 3.3–9.1-fold higher risk of accelerated brain aging than clinical diagnoses alone, operating through systemic inflammation, epigenetic alterations, and allostatic load [225]—the same upstream inputs that feed the SASP→STAT3 axis described here. When the instructor fails, the source is never removed, and every tissue falls into its own trap. A third layer of DC incompetence compounds the epigenetic and metabolic failures: Schaupp demonstrated in Cell that the microbiome controls constitutive type I IFN production by plasmacytoid DCs, which instructs a poised basal state in conventional DCs required for rapid pathogen responses [235]—aging-associated dysbiosis reduces this tonic IFN-I signal, leaving endogenous DCs unpoised even before IRF8 silencing and metabolic collapse take hold. The alpha-DC1 bypasses this because its manufacturing cocktail provides exogenous IFN-α, artificially supplying the poising signal the aged microbiome can no longer deliver. The tolerogenic default is therefore not a single pathway failure but a systems-level phase transition. Every major signaling axis in the DC has a binary immunogenic-versus-tolerogenic output, and IRF8 silencing flips all of them simultaneously because IRF8 sits at their intersection. Hippo/MST1 kinases directly phosphorylate STAT3 at T622 to block dimerization—an endogenous brake released when Hippo declines with aging [226]; MST1/2 simultaneously maintains the oxidative phosphorylation required for IL-12 in cDC1s [145]. The circadian regulator BMAL1 directly programs IL-12 responses through rhythms in mitochondrial morphology and metabolism in DCs [227,228]—sleep disruption collapses this cycling, creating temporal windows of IL-12 incompetence that compound the epigenetic silencing. Wnt/β-catenin activation independently programs DCs to a tolerogenic state—inducing IL-10, TGF-β, and PD-L1 [229]—a parallel axis that converges with STAT3 but that the alpha-DC1's ex vivo manufacturing also excludes. Autocrine complement C5a amplifies IL-12 production in immunogenic DCs through C5aR but inverts to tolerogenic CREB/IL-10 signaling when IRF8 is silenced [230]. And the AhR-IDO loop deepens progressively as downstream kynurenine metabolites recruit additional coactivators (NCOA7), explaining why the default becomes harder to reverse with time [231]. The alpha-DC1 does not need to address each axis individually because restoring IRF8 in the correct chromatin context simultaneously resets all of them to their immunogenic state—a single manufactured cell correcting a systems-level failure installed by a single epigenetic event at a single locus. Alzheimer's disease illustrates this principle: the temporal code that governs the alpha-DC1's correction applies to IL-12 itself, where chronic IL-12 from IRF8-deficient microglia drives neuronal pathology [211,212] while pulsatile IL-12 from a correctly manufactured DC writes activation. The same signal heals or destroys depending entirely on duration and context.

The combination predictions generated by this framework are immediately testable. Alpha-DC1 plus EZH2 inhibitors should synergize through simultaneous dual-mark removal. Alpha-DC1 plus anti-CD47 should synergize because IRF8-restored DCs provide the STING scaffold that CD47 blockade requires for cGAS-dependent DNA sensing [104,203]. Alpha-DC1 plus rapamycin bridge therapy could lower the STAT3 field intensity before vaccination, creating a more permissive environment for the cascade to propagate. Each prediction is falsifiable, each involves approved or trial-stage agents, and each follows directly from the mechanistic architecture described here.

NAD+ supplementation illustrates both the power and the limitation of single-loop interventions. Wang and colleagues demonstrated that decreased NAD+ inactivates SIRT1, resulting in increased STAT3 acetylation and phosphorylation, and that NAD+ repletion reversed STAT3 activation—Loop 3 operating in real time [216]. Critically, NAD+ decline also triggered IL-6 and TGF-β secretion—two of the nine STAT3 inputs—meaning NAD+ depletion actively amplifies the

© 2026 by the author(s). Distributed under a Creative Commons CC BY license.

Preprints.org (www.preprints.org) | NOT PEER-REVIEWED | Posted: 15 April 2026 doi:10.20944/preprints202604.0868.v2

tolerogenic default rather than merely failing to brake it. Minhas and colleagues showed aged macrophages paradoxically suppress de novo NAD+ synthesis despite upstream pathway activation, and that restoring NAD+ generation rescued oxidative phosphorylation and immune function [217]. However, NAD+ cannot reverse DNA methylation already installed at the IRF8 promoter: the MBD1/PIAS1 barrier [34] is not NAD+-dependent, and the SIRT1-DNMT1 relationship is paradoxically bidirectional—SIRT1 is required for initial DNMT3B recruitment to damaged promoters and can maintain silencing at already-methylated loci [218,219]. The framework predicts NAD+ supplementation (NMN/NR) is most valuable as maintenance therapy after alpha-DC1 correction—sustaining the restored SIRT1 brake on STAT3 to prevent re-establishment of the tolerogenic default, while the cascade has already cleared the epigenetic locks that NAD+ alone cannot reverse.

6.6. Conclusion

Immune failure is not a deficit of effector capacity. It is a failure of instruction. The mechanism chain is not linear but a closed causal loop (Figure 3): IRF8 silencing produces immune failure that allows senescent cells to accumulate, producing more SASP that silences more IRF8. Iron accumulation in senescent cells fuels ACSL4-dependent lipid peroxidation that generates additional senescent cells while simultaneously producing oxidized phospholipids that suppress IL-12 and reactive oxygen species that recruit DNMT1 to CpG island promoters independently of STAT3, creating parallel metabolic entry points into the silencing chain. Ovadya demonstrated directly that impaired cytotoxic immune function accelerates senescent cell accumulation and aging in vivo [195]. NK cells, whose function depends on IRF8-controlled IL-12/STAT4 signaling, are primary executors of senescent cell clearance through perforin-granzyme exocytosis [196]. The mechanistic chain is now traceable at every node. The human perforin gene is a direct STAT4 target, with tandem STAT-binding sequences in the perforin promoter requiring STAT4 homo-tetramer binding for IL-12-induced transcription [251]. When IRF8 is silenced and IL-12 lost, STAT4 is inactive and perforin transcription fails. Critically, aged NK cells retain normal intracellular perforin and granzyme B levels but fail to release them due to defective polarization of lytic granules toward the immunological synapse—a post-binding, post-activation delivery defect caused by Cdc42 GTPase overactivation [252,253]. Sagiv and colleagues proved that granule exocytosis, not death-receptor-mediated apoptosis, is the required pathway for NK-mediated senescent cell killing [254]. The defect is environmental, not cell-intrinsic: aged NK cells transferred into young mice regain function, while young NK cells in aged hosts lose it—and IL-15 receptor agonists completely reverse the deficiency [255,256]. IL-12 directly enhances NK cell granule exocytosis through Ca2+-dependent signaling [257], and aged NK cells retain the capacity to respond to IL-12 stimulation [258]. The alpha-DC1's IL-12 delivery therefore addresses the exact mechanism that fails: not NK cell depletion, but the loss of the instructional signal required to deploy a killing machinery that remains intact. The alpha-DC1 is therefore not merely an immunotherapy. It is a biological senolytic: an intervention that clears senescent cells not pharmacologically but by restoring the immune system's endogenous capacity to clear them, thereby removing the upstream cause of its own necessity. The alpha-DC1 simultaneously restores all ten IRF8-dependent surveillance functions, breaks all seven self-reinforcing feedback loops by removing their SASP input, unlocks IL-12 from all seven molecular locks through ex vivo manufacturing outside the STAT3 field, and reverses all three dimensions of bilateral disarmament—immune, metabolic, and target—through a single manufactured cell that renders itself unnecessary by correcting the upstream cause of its own requirement. Senolytics clear senescent cells but cannot restore the surveillance system preventing reaccumulation. The alpha-DC1 restores the surveillance system itself. Aging is not an accumulation of damage. It is the consequence of the quality control system's failure to clear the damage—a failure driven by one epigenetic event at one locus, reversible by one manufactured cell.

© 2026 by the author(s). Distributed under a Creative Commons CC BY license.

Preprints.org (www.preprints.org) | NOT PEER-REVIEWED | Posted: 15 April 2026 doi:10.20944/preprints202604.0868.v2

Figure 3. The Complete Biological Reboot Circuit: From Tolerogenic Default to Durable Immune Restoration

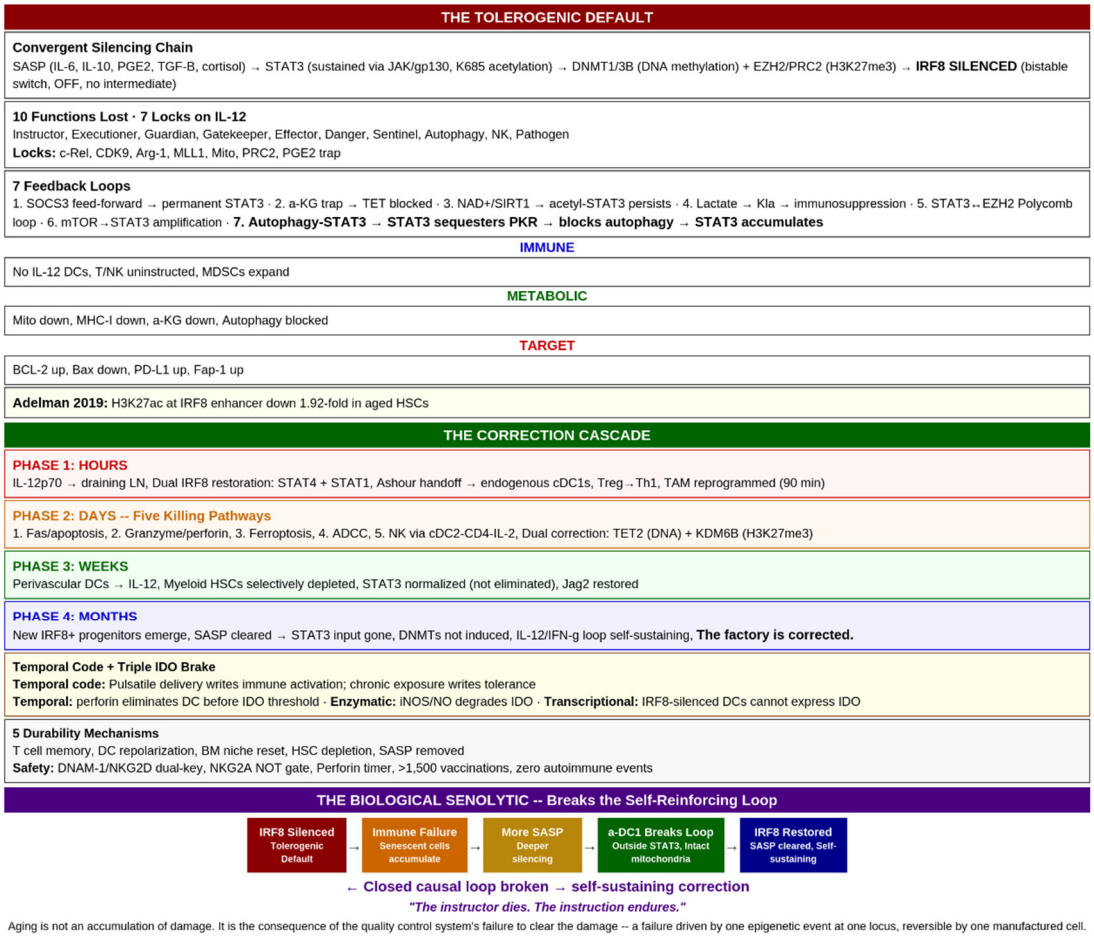

Figure 3. The complete biological reboot circuit: from tolerogenic default to durable immune restoration. Integrated overview showing the tolerogenic default (left) and the alpha-DC1 correction cascade (right) as two states of a single bidirectional circuit. The tolerogenic default installs bilateral disarmament through the SASP–STAT3–DNMT/EZH2–IRF8 silencing chain, locked by seven molecular locks on IL-12 and seven self-reinforcing feedback loops. The alpha-DC1, manufactured outside the STAT3 field with restored IRF8 and intact mitochondria, breaks the closed causal loop through a four-phase cascade constrained by the temporal code: pulsatile delivery writes immune activation while chronic exposure writes tolerance. Three hierarchical brakes prevent IDO-mediated counter-regulation. Five durability mechanisms ensure the corrected state persists after the alpha-DC1 is eliminated. The circuit resolves to a self-sustaining state in which the alpha-DC1 is no longer needed.

© 2026 by the author(s). Distributed under a Creative Commons CC BY license.

Preprints.org (www.preprints.org) | NOT PEER-REVIEWED | Posted: 15 April 2026 doi:10.20944/preprints202604.0868.v2

Figure 4. The Self-Reinforcing Trap: Seven Feedback Loops Lock the Tolerogenic Default

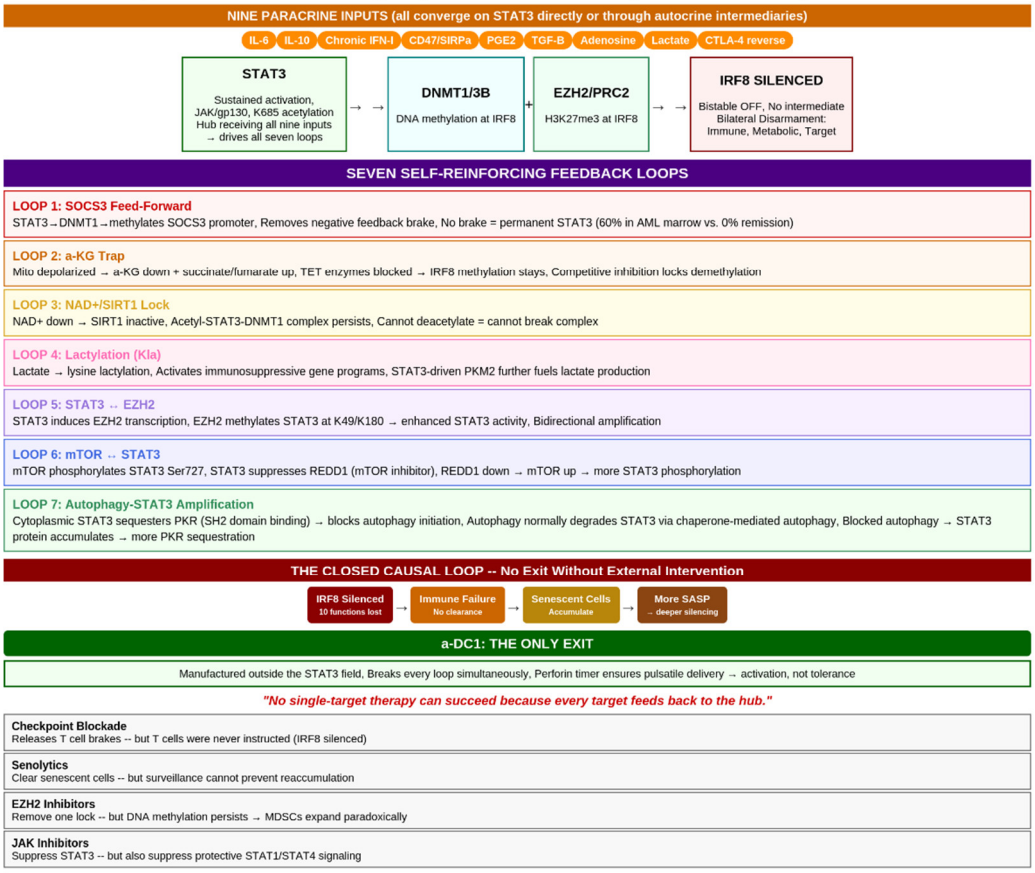

Figure 4. The self-reinforcing trap: seven feedback loops lock the tolerogenic default. STAT3 serves as the central hub receiving nine paracrine inputs and driving seven self-reinforcing feedback loops that collectively ensure the tolerogenic default cannot self-correct. Loop 1 (SOCS3 feed-forward): STAT3-induced DNMT1 methylates the SOCS3 promoter, removing the negative feedback brake. Loop 2 (α-KG trap): mitochondrial depolarization depletes the TET cofactor α-ketoglutarate while competitive inhibitors accumulate. Loop 3 (NAD+/SIRT1 lock): declining NAD+ inactivates the STAT3 deacetylase SIRT1, preserving the acetylated STAT3-DNMT1 complex. Loop 4 (lactylation): tumor-derived lactate drives lysine lactylation activating immunosuppressive programs. Loop 5 (Polycomb): STAT3 and EZH2 bidirectionally amplify each other. Loop 6 (mTOR amplification): mTOR phosphorylates STAT3 at Ser727 while STAT3 suppresses the mTOR inhibitor REDD1. The closed causal loop at the bottom shows how the output (immune failure → senescent cell accumulation → more SASP) feeds back to the input (more STAT3 activation → deeper IRF8 silencing). Loop 7 (autophagy-STAT3 amplification): cytoplasmic STAT3 directly sequesters PKR through SH2 domain binding, blocking autophagy initiation; autophagy normally degrades activated STAT3 through chaperone-mediated autophagy, so its inhibition causes STAT3 protein accumulation—a protein-level lock distinct from the epigenetic and metabolic locks above. This creates a selective autophagy dissociation: IRF8-dependent immune cell autophagy is OFF (no pathogen clearance, no debris processing, no TLR-to-IL-12 amplification), AMPK-dependent MHC-I autophagy is ON (cross-presentation collapses), and senescent cell-intrinsic autophagy is REPROGRAMMED to sustain SASP production—the worst of all three states simultaneously. No single-target therapy can exit this trap because every target feeds back to the STAT3 hub. The alpha-DC1, manufactured outside the field, is the only intervention that breaks all seven loops simultaneously.

Author Contributions: AC: Conceptualization, Writing – original draft, Writing – review and editing. AB: Writing – review and editing.

Funding: This work received no external funding.

Institutional Review Board Statement: This project was exempt from IRB review as it did not qualify as human subject research under federal regulations.

© 2026 by the author(s). Distributed under a Creative Commons CC BY license.

Preprints.org (www.preprints.org) | NOT PEER-REVIEWED | Posted: 15 April 2026 doi:10.20944/preprints202604.0868.v2

Data Availability Statement: No datasets were generated or analyzed for this study.

Acknowledgments: During the preparation of this manuscript, the authors used multiple AI-assisted tools for literature search, reference verification, manuscript drafting, and iterative editing: Claude (Anthropic, Claude Opus 4 / Claude Opus 4.6) for research synthesis and manuscript composition; Perplexity (Perplexity AI, Inc.) and OpenEvidence for literature search and reference verification; Gemini (Google, Gemini 2.5 Pro) for supplementary research; Grok (xAI) and ChatGPT (OpenAI, GPT-4o) for cross-validation. All scientific claims, interpretations, and arguments were directed, reviewed, and verified by the authors, who take full responsibility for the accuracy and content of the final published text.

Conflicts of Interest Statement: Author AC has filed a provisional patent application covering methods and compositions related to concepts described in this manuscript. AB is affiliated with SaltusBiotech.

Abbreviations

DC, dendritic cell; alpha-DC1, alpha-type-1 polarized dendritic cell; SASP, senescence-associated secretory phenotype; IRF8, interferon regulatory factor 8; STAT3, signal transducer and activator of transcription 3; DNMT, DNA methyltransferase; MDSC, myeloid-derived suppressor cell; Treg, regulatory T cell; IFN, interferon; IL, interleukin; PGE2, prostaglandin E2; TLR, Toll-like receptor; BCG, Bacillus Calmette-Guérin; HSC, hematopoietic stem cell; cDC1, conventional type 1 dendritic cell; OPA1, optic atrophy 1; AMPK, AMP-activated protein kinase; NAD+, nicotinamide adenine dinucleotide; SIRT1, sirtuin 1; TET, ten-eleven translocation; α-KG, alpha-ketoglutarate; CHIP, clonal hematopoiesis of indeterminate potential; SOCS3, suppressor of cytokine signaling 3; Kla, lysine lactylation; PD-L1, programmed death-ligand 1; TMRM, tetramethylrhodamine methyl ester.

References

1. 1. Steinman RM, Cohn ZA. Identification of a novel cell type in peripheral lymphoid organs of mice. J Exp Med (1973) 137:1142–1162. doi: 10.1084/jem.137.5.1142
2. 2. Banchereau J, Steinman RM. Dendritic cells and the control of immunity. Nature (1998) 392:245–252. doi: 10.1038/32588
3. 3. Hawiger D, Inaba K, Dorsett Y, et al. Dendritic cells induce peripheral T cell unresponsiveness under steady state conditions in vivo. J Exp Med (2001) 194:769–779. doi: 10.1084/jem.194.6.769
4. 4. Krummel MF, Allison JP. CD28 and CTLA-4 have opposing effects on the response of T cells to stimulation. J Exp Med (1995) 182:459–465. doi: 10.1084/jem.182.2.459
5. 5. Leach DR, Krummel MF, Allison JP. Enhancement of antitumor immunity by CTLA-4 blockade. Science (1996) 271:1734–1736. doi: 10.1126/science.271.5256.1734
6. 6. Sakaguchi S, Sakaguchi N, Asano M, et al. Immunologic self-tolerance maintained by activated T cells expressing IL-2 receptor alpha-chains (CD25). J Immunol (1995) 155:1151–1164.
7. 7. Hori S, Nomura T, Sakaguchi S. Control of regulatory T cell development by the transcription factor Foxp3. Science (2003) 299:1057–1061. doi: 10.1126/science.1079490
8. 8. Wing K, Onishi Y, Prieto-Martin P, et al. CTLA-4 control over Foxp3+ regulatory T cell function. Science (2008) 322:271–275. doi: 10.1126/science.1160062
9. 9. Qureshi OS, Zheng Y, Nakamura K, et al. Trans-endocytosis of CD80 and CD86: a molecular basis for the cell-extrinsic function of CTLA-4. Science (2011) 333:261–263. doi: 10.1126/science.1202947
10. 10. Kennedy A, Waters E, Rowshanravan B, et al. Differences in CD80 and CD86 transendocytosis reveal CD86 as a key target for CTLA-4 immune regulation. Nat Immunol (2022) 23:1365–1378. doi: 10.1038/s41590-022-01289-w
11. 11. Mailliard RB, Wieckowski E, Muthuswamy R, et al. Alpha-type-1 polarized dendritic cells: a novel immunization tool with optimized CTL-inducing activity. Cancer Res (2004) 64:5934–5937. doi: 10.1158/0008-5472.CAN-04-1261

© 2026 by the author(s). Distributed under a Creative Commons CC BY license.

Preprints.org (www.preprints.org) | NOT PEER-REVIEWED | Posted: 15 April 2026 doi:10.20944/preprints202604.0868.v2

12. 12. Hansen M, Hjorto GM, Donia M, et al. Comparison of clinical grade type 1-polarized and standard matured dendritic cells for cancer immunotherapy. Vaccine (2013) 31:639–646. doi: 10.1016/j.vaccine.2012.11.063
13. 13. Dong H, Obermajer N, Tsuji T, et al. Contributions of DNAM-1 and NKG2D to functional activation of human CTLs. Cancer Immunol Res (2024) 12:339–353. doi: 10.1158/2326-6066.CIR-23-0245
14. 14. Feng T, Cao AT, Weaver CT, et al. Interleukin-12 converts Foxp3+ regulatory T cells to interferon-gamma-producing Foxp3+ T cells that inhibit colitis. Gastroenterology (2011) 140:2031–2043. doi: 10.1053/j.gastro.2011.03.009
15. 15. Wilson CB, Makar KW, Shnyreva M, et al. DNA methylation and the expanding epigenetics of T cell lineage commitment. Semin Immunol (2005) 17:105–119. doi: 10.1016/j.smim.2005.01.005
16. 16. Qiao Y, Giannopoulou EG, Chan CH, et al. Synergistic activation of inflammatory cytokine genes by interferon-gamma-induced chromatin remodeling and toll-like receptor signaling. Immunity (2013) 39:454–469. doi: 10.1016/j.immuni.2013.08.009
17. 17. Ostuni R, Piccolo V, Barozzi I, et al. Latent enhancers activated by stimulation in differentiated cells. Cell (2013) 152:157–171. doi: 10.1016/j.cell.2012.12.018
18. 18. Mikulski P, Schubert S, Giesselmann S, et al. IFN-gamma-induced chromatin memory in human cells is maintained through mitotic divisions by the histone acetyltransferase KAT7. Nat Struct Mol Biol (2025) 32:512–523. doi: 10.1038/s41594-024-01437-4
19. 19. Cowley CJ, Sajjath SM, Soto-Ugaldi LF, et al. Distinctive DNA sequence features define epigenetic longevity of inflammatory memory. Science (2026) 391(6792):1347–1354.
20. 20. Subbiah V, Murthy R, Hong DS, et al. Cytokines produced by dendritic cells administered intratumorally correlate with clinical outcome in patients with diverse cancers. Clin Cancer Res (2018) 24:3845–3856. doi: 10.1158/1078-0432.CCR-17-2707
21. 21. Liau LM, Ashkan K, Brem S, et al. Association of autologous tumor lysate-loaded dendritic cell vaccination with extension of survival among patients with newly diagnosed and recurrent glioblastoma. JAMA Oncol (2023) 9:112–121. doi: 10.1001/jamaoncol.2022.5370
22. 22. Jackson AL, Matsumoto H, Janszen M, et al. Restricted expression of p55 interleukin 2 receptor (CD25) on normal T cells. Clin Immunol Immunopathol (1990) 54:126–133. doi: 10.1016/0090-1229(90)90012-F
23. 23. Coppe JP, Patil CK, Rodier F, et al. Senescence-associated secretory phenotypes reveal cell nonautonomous functions of oncogenic RAS and the p53 tumor suppressor. PLoS Biol (2008) 6:e301. doi: 10.1371/journal.pbio.0060301
24. 24. Manz MG, Boettcher S. Emergency granulopoiesis. Nat Rev Immunol (2014) 14:302–314. doi: 10.1038/nri3660
25. 25. Park SJ, Nakagawa T, Kitamura H, et al. IL-6 regulates in vivo dendritic cell differentiation through STAT3 activation. J Immunol (2004) 173:3844–3854. doi: 10.4049/jimmunol.173.6.3844
26. 26. Kalinski P, Hilkens CM, Snijders A, et al. IL-12-deficient dendritic cells, generated in the presence of prostaglandin E2, promote type 2 cytokine production in maturing human naive T helper cells. J Immunol (1997) 159:28–35.
27. 27. Gabrilovich DI, Nagaraj S. Myeloid-derived suppressor cells as regulators of the immune system. Nat Rev Immunol (2009) 9:162–174. doi:10.1038/nri2506
28. 28. Spranger S, Bao R, Gajewski TF. Melanoma-intrinsic beta-catenin signalling prevents anti-tumour immunity. Nature (2015) 523:231–235. doi: 10.1038/nature14404
29. 29. Goriely S, Demonte D, Ziegler-Heitbrock L, et al. Human IL-12(p35) gene activation involves selective remodeling of a single nucleosome within a region of the promoter containing critical Sp1-binding sites. Blood (2003) 101:4894–4902. doi: 10.1182/blood-2002-09-2851
30. 30. Tamura T, Yanai H, Savitsky D, et al. The IRF family transcription factors in immunity and oncogenesis. Annu Rev Immunol (2008) 26:535–584. doi: 10.1146/annurev.immunol.26.021607.090400
31. 31. Salem S, Salem D, Gros P. Role of IRF8 in immune cells functions, protection against infections, and susceptibility to inflammatory diseases. Hum Genet (2020) 139:707–721. doi: 10.1007/s00439-020-02154-2

© 2026 by the author(s). Distributed under a Creative Commons CC BY license.

Preprints.org (www.preprints.org) | NOT PEER-REVIEWED | Posted: 15 April 2026 doi:10.20944/preprints202604.0868.v2

32. 32. Langlais D, Barreiro LB, Gros P. The macrophage IRF8/IRF1 regulome is required for protection against infections and is associated with chronic inflammation. J Exp Med (2016) 213:585–603. doi:10.1084/jem.20151764
33. 33. Ibrahim ML, Klement JD, Lu C, et al. Myeloid-derived suppressor cells produce IL-10 to elicit DNMT3b-dependent IRF8 silencing to promote colitis-associated colon tumorigenesis. Cell Rep (2018) 25:3036–3046.e6. doi: 10.1016/j.celrep.2018.11.050
34. 34. McGough JM, Yang D, Huang S, et al. DNA methylation represses IFN-gamma-induced and signal transducer and activator of transcription 1-mediated IFN regulatory factor 8 activation in colon carcinoma cells. Mol Cancer Res (2008) 6:1841–1851. doi: 10.1158/1541-7786.MCR-08-0280
35. 35. Ohno Y, Kitamura H, Takahashi N, et al. IL-6 down-regulates HLA class II expression and IL-12 production of human dendritic cells to impair activation of antigen-specific CD4+ T cells. Cancer Immunol Immunother (2016) 65:193–204. doi: 10.1007/s00262-015-1791-9
36. 36. Pathak S, Ma S, Shukla V, et al. A role for IRF8 in B cell anergy. J Immunol (2013) 191:6222–6230. doi: 10.4049/jimmunol.1301169
37. 37. Zhao B, Takami M, Yamada A, et al. Interferon regulatory factor-8 regulates bone metabolism by suppressing osteoclastogenesis. Nat Med (2009) 15:1066–1071. doi: 10.1038/nm.2007
38. 38. Lung TL, Saurwein-Teissl M, Parson W, et al. Unimpaired dendritic cells can be derived from monocytes in old age and can mobilize residual function in senescent T cells. Vaccine (2000) 18:1606–1612. doi:10.1016/S0264-410X(99)00494-6
39. 39. Zhou J, Tison K, Zhou H, et al. STAT5 and STAT3 balance shapes dendritic cell function and tumour immunity. Nature (2025) 643:519–528.
40. 40. Zhivaki D, Kennedy SN, Park J, et al. Correction of age-associated defects in dendritic cells enables CD4+ T cells to eradicate tumors. Cell (2024) 187:3888–3903.e18. doi: 10.1016/j.cell.2024.05.026
41. 41. Tsuji S, Matsumoto M, Takeuchi O, et al. Maturation of human dendritic cells by cell wall skeleton of Mycobacterium bovis bacillus Calmette-Guerin: involvement of toll-like receptors. Infect Immun (2000) 68:6883–6890. doi: 10.1128/IAI.68.12.6883-6890.2000
42. 42. Shankar G, Pestano LA, Bosch ML. Interferon-gamma added during bacillus Calmette-Guerin induced dendritic cell maturation stimulates potent Th1 immune responses. J Transl Med (2003) 1:7. doi:10.1186/1479-5876-1-7
43. 43. Chang TH, Xu S, Tailor P, et al. The small ubiquitin-like modifier-deconjugating enzyme sentrin-specific peptidase 1 switches IFN regulatory factor 8 from a repressor to an activator during macrophage activation. J Immunol (2012) 189:3548–3556. doi:10.4049/jimmunol.1201104
44. 44. Fesneau O, Theate I, Caux C, et al. IL-12 drives NKG2A expression on tumor-reactive CD8+ T cells. Immunity (2024) 57:1614–1631.
45. 45. Ashour D, Arampatzi P, Pavlovic V, et al. IL-12 from endogenous cDC1, and not vaccine DC, is required for Th1 induction. J Clin Invest (2020) 130:3051–3060. doi: 10.1172/JCI125938
46. 46. Matatall KA, Jeong M, Chen S, et al. Chronic infection depletes hematopoietic stem cells through stress-induced terminal differentiation. Cell Rep (2016) 17:2584–2595. doi:10.1016/j.celrep.2016.11.031
47. 47. Panda A, Qian F, Mohanty S, et al. Age-associated decrease in TLR function in primary human dendritic cells predicts influenza vaccine response. J Immunol (2010) 184:2518–2527. doi: 10.4049/jimmunol.0901872
48. 48. Compte N, Zouaoui Boudjeltia K, Vanhaeverbeek M, et al. Frailty in old age is associated with decreased interleukin-12/23 production in response to toll-like receptor ligation. PLoS One (2013) 8:e65325. doi:10.1371/journal.pone.0065325
49. 49. Guo Z, Tilburgs T, Wong B, et al. Dysfunction of dendritic cells in aged C57BL/6 mice leads to failure of natural killer cell activation and of tumor eradication. Proc Natl Acad Sci U S A (2014) 111:14199–14204. doi: 10.1073/pnas.1414780111
50. 50. Wagner AH, Conzelmann M, Fitzer F, et al. JAK1/STAT3 activation directly inhibits IL-12 production in dendritic cells by preventing CDK9/P-TEFb recruitment to the p35 promoter. Biochem Pharmacol (2015) 96:52–64. doi: 10.1016/j.bcp.2015.04.019

© 2026 by the author(s). Distributed under a Creative Commons CC BY license.

Preprints.org (www.preprints.org) | NOT PEER-REVIEWED | Posted: 15 April 2026 doi:10.20944/preprints202604.0868.v2

51. 51. Kim D, Park G, Huuhtanen J, et al. STAT3 activation in large granular lymphocyte leukemia is associated with cytokine signaling and DNA hypermethylation. Leukemia (2021) 35:3430–3443. doi:10.1038/s41375-021-01256-6
52. 52. Rojas-Canales D, Krishnan R, Jessup CF, et al. Early exposure of interferon-gamma inhibits signal transducer and activator of transcription-6 signalling and nuclear factor kappaB activation in a short-term monocyte-derived dendritic cell culture promoting regulatory dendritic cells. Clin Exp Immunol (2012) 167:447–458. doi:10.1111/j.1365-2249.2011.04521.x
53. 53. Smith AM, Qualls JE, O'Brien K, et al. A distal enhancer in Il12b is the target of transcriptional repression by the STAT3 pathway and requires the basic leucine zipper (B-ZIP) protein NFIL3. J Biol Chem (2011) 286:23582–23590. doi: 10.1074/jbc.M111.249235
54. 54. Hoentjen F, Sartor RB, Ozaki M, et al. STAT3 regulates NF-kappaB recruitment to the IL-12p40 promoter in dendritic cells. Blood (2005) 105:689–696. doi: 10.1182/blood-2004-05-2042
55. 55. Molony RD, Nguyen JT, Kong Y, et al. Aging impairs both primary and secondary RIG-I signaling for interferon induction in human monocytes. Sci Signal (2017) 10(509):eaan2392. doi: 10.1126/scisignal.aan2392
56. 56. Zhang Z, Huang X, Wang E, et al. Suppression of Mll1-complex by Stat3/Cebpbeta-induced miR-21a/21b/181b maintains the accumulation, homeostasis, and immunosuppressive function of polymorphonuclear myeloid-derived suppressor cells. J Immunol (2020) 204:3400–3415. doi:10.4049/jimmunol.2000230
57. 57. Zaccard CR, Watkins SC, Kalinski P, et al. CD40L induces functional tunneling nanotube networks exclusively in dendritic cells programmed by mediators of type 1 immunity. J Immunol (2015) 194:1047–1056. doi:10.4049/jimmunol.1401832
58. 58. Wang W, Green M, Choi JE, et al. CD8+ T cells regulate tumour ferroptosis during cancer immunotherapy. Nature (2019) 569:270–274. doi:10.1038/s41586-019-1170-y
59. 59. Ferris ST, Ohara RA, Ou F, et al. cDC1 vaccines drive tumor rejection by direct presentation independently of host cDC1. Cancer Immunol Res (2022) 10:920–931. doi: 10.1158/2326-6066.CIR-21-0804
60. 60. Khateb M, Azriel A, Levi BZ. The third intron of IRF8 is a cell-type-specific chromatin priming element during mouse embryonal stem cell differentiation. J Mol Biol (2019) 431:210–222. doi:10.1016/j.jmb.2018.11.022
61. 61. Politis AD, Sivo J, Driggers PH, et al. Modulation of interferon consensus sequence binding protein mRNA in murine peritoneal macrophages. J Immunol (1992) 148:801–22429.
62. 62. Liu J, Guan X, Tamura T, Ozato K, Ma X. Synergistic activation of interleukin-12 p35 gene transcription by interferon regulatory factor-1 and interferon consensus sequence-binding protein. J Biol Chem (2004) 279:55609–55617. doi: 10.1074/jbc.M407131200
63. 63. Lanca T, Ungerback J, Da Silva C, et al. IRF8 deficiency induces the transcriptional, functional, and epigenetic reprogramming of cDC1 into the cDC2 lineage. Immunity (2022) 55:1431–1447.e11. doi:10.1016/j.immuni.2022.06.006
64. 64. Burchert A, Cai D, Hofbauer LC, et al. Interferon consensus sequence binding protein (ICSBP; IRF-8) antagonizes BCR/ABL and down-regulates bcl-2. Blood (2004) 103:3480–3489. doi: 10.1182/blood-2003-08-2970
65. 65. Yang D, Thangaraju M, Green K, et al. IFN regulatory factor 8 sensitizes soft tissue sarcoma cells to death receptor-initiated apoptosis via repression of FLICE-like protein. Cancer Res (2009) 69:1080–1088. doi: 10.1158/0008-5472.CAN-08-2520
66. 66. Hu X, Yang D, Zimmerman M, et al. IRF8 regulates acid ceramidase expression to mediate apoptosis and suppresses tumourigenesis. Nat Commun (2011) 2:1–12. doi: 10.1038/ncomms1569
67. 67. Yang D, Wang S, Brooks C, et al. IFN regulatory factor 8 mediates apoptosis in nonhemopoietic tumor cells via regulation of Fas expression. J Immunol (2007) 179:4775–4782. doi:10.4049/jimmunol.179.7.4775
68. 68. Huang W, Zhu C, Wang H, et al. IRF8 represses PTPN13/FAP-1 expression and sensitizes tumor cells to FAS-mediated apoptosis. Cancer Immunol Res (2015) 3:73–83. doi: 10.1158/2326-6066.CIR-14-0094

© 2026 by the author(s). Distributed under a Creative Commons CC BY license.

Preprints.org (www.preprints.org) | NOT PEER-REVIEWED | Posted: 15 April 2026 doi:10.20944/preprints202604.0868.v2

69. 69. Kurotaki D, Yamamoto M, Nishiyama A, et al. IRF8 inhibits C/EBP-alpha activity to restrain mononuclear phagocyte progenitors from differentiating into neutrophils. Nat Commun (2014) 5:4978. doi:10.1038/ncomms5978
70. 70. Lee J, Zhou YJ, Ma W, et al. Lineage specification of human dendritic cells is marked by IRF8 expression in hematopoietic stem cells and multipotent progenitors. Nat Immunol (2017) 18:877–888. doi:10.1038/ni.3789
71. 71. Meyer MA, Baer JM, Knolhoff BL, et al. Breast and pancreatic cancer interrupt IRF8-dependent dendritic cell development to overcome immune surveillance. Nat Commun (2018) 9:1250. doi: 10.1038/s41467-018-03600-6
72. 72. Miyagawa F, Zhang H, Terunuma A, et al. Interferon regulatory factor 8 integrates T-cell receptor and cytokine-signaling pathways and drives effector differentiation of CD8 T cells. Proc Natl Acad Sci U S A (2012) 109:12123–12128. doi: 10.1073/pnas.1201453109
73. 73. Li R, Wei K, Sun Q, et al. Analysis of the three-dimensional genome of exhausted CD8+ T cells reveals a critical role of IRF8 in their differentiation and functions in cancer. Nat Immunol (2025) 26:2280–2295. doi: 10.1038/s41590-025-02330-4
74. 74. Luo W, Zou Z, Tao S, et al. IRF8 is associated with STING to modulate DNA damage-induced cellular senescence. Nat Commun (2023) 14:5504. doi: 10.1038/s41467-023-41053-6
75. 75. Zhao J, Kong HJ, Li H, et al. IRF-8/interferon (IFN) consensus sequence-binding protein is involved in Toll-like receptor (TLR) signaling and contributes to the cross-talk between TLR and IFN-gamma signaling pathways. J Biol Chem (2006) 281:10073–10080. doi:10.1074/jbc.M507788200
76. 76. Saeki K, Shichino S, Ueha S, et al. IRF8 configures enhancer landscape in postnatal microglia and directs microglia specific transcriptional programs. Nat Immunol (2024) 25:1928–1942. doi:10.1038/s41590-024-01962-2
77. 77. Yan J, Chen G, Tong S, et al. IRF8 contributes to mucosal immunity by promoting IFN-gamma expression in gastric epithelial cells. J Cell Biochem (2018) 119:1274–1281.
78. 78. Gupta M, Shin DM, Ramakrishna L, et al. IRF8 directs stress-induced autophagy in macrophages and promotes clearance of Listeria monocytogenes. Nat Commun (2015) 6:6379. doi: 10.1038/ncomms7379
79. 79. Adams NM, Lau CM, Fan X, et al. Transcription factor IRF8 orchestrates the adaptive natural killer cell response. Immunity (2018) 48:1172–1182.e6. doi: 10.1016/j.immuni.2018.04.018
80. 80. Mace EM, Bigley V, Gunesch JT, et al. Biallelic mutations in IRF8 impair human NK cell maturation and function. J Clin Invest (2017) 127:306–320. doi: 10.1172/JCI86276
81. 81. Alter-Koltunoff M, Goren S, Nousbeck J, et al. Innate immunity to intraphagosomal pathogens is mediated by interferon regulatory factor 8 (IRF-8) that stimulates the expression of macrophage-specific Nramp1 through antagonizing repression by c-Myc. J Biol Chem (2008) 283:2724–2733. doi: 10.1074/jbc.M707704200
82. 82. Marquis JF, Vachon V, Bhatt DL, et al. The IRF-8 regulome includes genome-wide enrichment for GBP and IRG family antimicrobial effectors. Eur J Immunol (2011) 41:3270–3282. doi: 10.1002/eji.201141510
83. 83. Murphy TL, Murphy KM. The making of a cDC1: precision programming of progenitor potential. Immunol Rev (2026) 337:e70081. doi:10.1111/imr.70081
84. 84. Lehtonen A, Lund R, Lahesmaa R, Julkunen I, Sareneva T, Matikainen S. IFN-alpha and IL-12 activate IFN regulatory factor 1 (IRF-1), IRF-4, and IRF-8 gene expression in human NK and T cells. Cytokine (2003) 24:81–90. doi: 10.1016/j.cyto.2003.07.001
85. 85. Zebley CC, Abdelsamed HA, Ghoneim HE, et al. Proinflammatory cytokines promote TET2-mediated DNA demethylation during CD8 T cell effector differentiation. Cell Rep (2021) 37:109796. doi:10.1016/j.celrep.2021.109796
86. 86. Stirewalt DL, Choi YE, Sharpless NE, et al. Decreased IRF8 expression found in aging hematopoietic progenitor/stem cells. Leukemia (2009) 23:391–393. doi: 10.1038/leu.2008.176
87. 87. Elsner RA, Smita S, Engiles JB, Shlomchik MJ. Coordinated regulation of extrafollicular B cell responses by IL-12 and IFN-gamma. Immunol Rev (2025) 329:e70027. doi: 10.1111/imr.70027

© 2026 by the author(s). Distributed under a Creative Commons CC BY license.

Preprints.org (www.preprints.org) | NOT PEER-REVIEWED | Posted: 15 April 2026 doi:10.20944/preprints202604.0868.v2

88. 88. Watkins SK, Egilmez NK, Suttles J, et al. IL-12 rapidly alters the functional profile of tumor-associated and tumor-infiltrating macrophages in vitro and in vivo. J Immunol (2007) 178:1357–1362. doi:10.4049/jimmunol.178.3.1357
89. 89. Ewen EM, Pahl JHW, Miller M, et al. KIR downregulation by IL-12/15/18 unleashes human NK cells from KIR/HLA-I inhibition and enhances killing of tumor cells. Eur J Immunol (2018) 48:355–365. doi:10.1002/eji.201747128
90. 90. Hambleton S, Salem S, Bustamante J, et al. IRF8 mutations and human dendritic-cell immunodeficiency. N Engl J Med (2011) 365:127–138. doi:10.1056/NEJMoa1100066
91. 91. Basrai S, Nofech-Mozes I, Detroja R, et al. Blood-based epigenetic instability linked to human aging and disease. Nat Commun (2026) 17:2754. doi: 10.1038/s41467-026-69430-z
92. 92. Zhang Q, Wang HY, Woetmann A, et al. STAT3 induces transcription of the DNA methyltransferase 1 gene (DNMT1) in malignant T lymphocytes. Blood (2006) 108:1058–1064. doi: 10.1182/blood-2005-08-007377
93. 93. Li Q, Harden JL, Anderson CD, Egilmez NK. Tolerogenic phenotype of IFN-gamma-induced IDO+ dendritic cells is maintained via an autocrine IDO-kynurenine/AhR-IDO loop. J Immunol (2016) 197:962–970. doi:10.4049/jimmunol.1502615
94. 94. Edelstein MP, Ozaki Y, Duch DS. Synergistic effects of phorbol ester and IFN-gamma on the induction of indoleamine 2,3-dioxygenase in THP-1 monocytic leukemia cells. J Immunol (1989) 143:2969–2973.
95. 95. Kowalczyk A, D'Souza CA, Zhang L. Cell-extrinsic CTLA4-mediated regulation of dendritic cell maturation depends on STAT3. Eur J Immunol (2014) 44:1143–1155. doi: 10.1002/eji.201343601
96. 96. Yang J, Huck SP, McHugh RS, Hermans IF, Ronchese F. Perforin-dependent elimination of dendritic cells regulates the expansion of antigen-specific CD8+ T cells in vivo. Proc Natl Acad Sci U S A (2006) 103:147–152. doi: 10.1073/pnas.0509054103
97. 97. Chen M, Felix K, Wang J. Critical role for perforin and Fas-dependent killing of dendritic cells in the control of inflammation. Blood (2012) 119:127–136. doi: 10.1182/blood-2011-06-363994
98. 98. Harden JL, Gu T, Kilinc MO, et al. Dichotomous effects of IFN-gamma on dendritic cell function determine the extent of IL-12-driven antitumor T cell immunity. J Immunol (2011) 187:126–132. doi:10.4049/jimmunol.1100168
99. 99. Greeneltch KM, Schneider M, Steinberg SM, et al. Host immunosurveillance controls tumor growth via IFN regulatory factor-8 dependent mechanisms. Cancer Res (2007) 67:10406–10416. doi:10.1158/0008-5472.CAN-07-1228
100. 100. Hu X, Bardhan K, Paschall AV, et al. Deregulation of apoptotic factors Bcl-xL and Bax confers apoptotic resistance to myeloid-derived suppressor cells and contributes to their persistence in cancer. J Biol Chem (2013) 288:19103–19115. doi: 10.1074/jbc.M112.434530
101. 101. Mattei F, Schiavoni G, Sestili P, et al. IRF-8 controls melanoma progression by regulating the cross talk between cancer and immune cells within the tumor microenvironment. Neoplasia (2012) 14:1223–1235. doi:10.1593/neo.121444
102. 102. Montoya M, Collins SA, Chuntova P, et al. Interferon regulatory factor 8-driven reprogramming of the immune microenvironment enhances antitumor adaptive immunity and reduces immunosuppression in murine glioblastoma. Neuro-Oncology (2024) 26:2272–2287. doi:10.1093/neuonc/noae149
103. 103. Yang D, Thangaraju M, Greeneltch K, et al. Repression of IFN regulatory factor 8 by DNA methylation is a molecular determinant of apoptotic resistance and metastatic phenotype in metastatic tumor cells. Cancer Res (2007) 67:3301–3309. doi: 10.1158/0008-5472.CAN-06-4068
104. 104. Luo WW, Tong Z, Cao P, et al. Transcription-independent regulation of STING activation and innate immune responses by IRF8 in monocytes. Nat Commun (2022) 13:4822. doi: 10.1038/s41467-022-32401-1
105. 105. Braun DA, Fribourg M, Sealfon SC. Cytokine response is determined by duration of receptor and signal transducers and activators of transcription 3 (STAT3) activation. J Biol Chem (2013) 288:2986–2993. doi: 10.1074/jbc.M112.386573
106. 106. Qing Y, Stark GR. Alternative activation of STAT1 and STAT3 in response to interferon-gamma. J Biol Chem (2004) 279:41679–41685. doi:10.1074/jbc.M406413200

© 2026 by the author(s). Distributed under a Creative Commons CC BY license.

Preprints.org (www.preprints.org) | NOT PEER-REVIEWED | Posted: 15 April 2026 doi:10.20944/preprints202604.0868.v2

107. 107. Dees C, Pötter S, Zhang Y, et al. TGF-beta-induced epigenetic deregulation of SOCS3 facilitates STAT3 signaling to promote fibrosis. J Clin Invest (2020) 130:2347–2363. doi: 10.1172/JCI122462
108. 108. Zhao B, Takami M, Yamada A, et al. Interferon regulatory factor-8 regulates bone metabolism by suppressing osteoclastogenesis. Nat Med (2009) 15:1066–1071. doi: 10.1038/nm.2007
109. 109. Li CC, Munitic I, Mittelstadt PR, et al. Suppression of dendritic cell-derived IL-12 by endogenous glucocorticoids is protective in LPS-induced sepsis. PLoS Biol (2015) 13:e1002269. doi:10.1371/journal.pbio.1002269
110. 110. Soulier A, Blois SM, Sivakumaran S, et al. Cell-intrinsic regulation of murine dendritic cell function and survival by prereceptor amplification of glucocorticoid. Blood (2013) 122:3288–3297. doi:10.1182/blood-2013-03-489138
111. 111. Murphy TL, Murphy KM. The making of a cDC1: precision programming of progenitor potential. Immunol Rev (2026) 337:e70081. doi:10.1111/imr.70081
112. 112. Liu TT, Kim S, Desai P, et al. Ablation of cDC2 development by triple mutations within the Zeb2 enhancer. Nature (2022) 607:142–148. doi: 10.1038/s41586-022-04866-z
113. 113. Lee H, Zhang P, Herrmann A, et al. Acetylated STAT3 is crucial for methylation of tumor-suppressor gene promoters and inhibition by resveratrol results in demethylation. Proc Natl Acad Sci U S A (2012) 109:7765–7769. doi: 10.1073/pnas.1205132109
114. 114. Li Y, Deuring J, Peppelenbosch MP, et al. IL-6-induced DNMT1 activity mediates SOCS3 promoter hypermethylation in ulcerative colitis-related colorectal cancer. Carcinogenesis (2012) 33:1889–1896. doi: 10.1093/carcin/bgs214
115. 115. Zhang X, Zhang K, Zhang J, et al. DNMTs-mediated SOCS3 methylation promotes the occurrence and development of AML. Eur J Haematol (2024) 112:439–449. doi: 10.1111/ejh.14134
116. 116. Thomas SR, Mohr D, Stocker R. Nitric oxide inhibits indoleamine 2,3-dioxygenase activity in interferon-gamma primed mononuclear phagocytes. J Biol Chem (1994) 269:14457–14464.
117. 117. Hucke C, MacKenzie CR, Adjogble KD, et al. Nitric oxide-mediated regulation of gamma interferon-induced bacteriostasis: inhibition and degradation of human indoleamine 2,3-dioxygenase. Infect Immun (2004) 72:2723–2730. doi: 10.1128/IAI.72.5.2723-2730.2004
118. 118. López AS, Alegre E, Díaz A, et al. Bimodal effect of nitric oxide in the enzymatic activity of indoleamine 2,3-dioxygenase in human monocytic cells. Immunol Lett (2006) 106:163–171. doi:10.1016/j.imlet.2006.05.008
119. 119. Egilmez NK, Harden JL, Virtuoso LP, et al. Nitric oxide short-circuits interleukin-12-mediated tumor regression. Cancer Immunol Immunother (2011) 60:839–845. doi: 10.1007/s00262-011-0998-2
120. 120. Zhu J, Huang X, Yang G. Autocrine IL6-mediated activation of the STAT3–DNMT axis silences the TNF-alpha–RIP1 necroptosis pathway to sustain survival and accumulation of myeloid-derived suppressor cells. Cancer Res (2020) 80:3145–3156. doi: 10.1158/0008-5472.CAN-19-3458
121. 121. Matatall KA, Shen CC, Challen GA, King KY. Type II interferon promotes differentiation of myeloid-biased hematopoietic stem cells. Stem Cells (2014) 32:3023–3030. doi: 10.1002/stem.1799
122. 122. Patel B, Zhou Y, Babcock RL, et al. STAT3 protects hematopoietic stem cells by preventing activation of a deleterious autocrine type-I interferon response. Leukemia (2024) 38:1143–1155. doi:10.1038/s41375-024-02218-6
123. 123. Mantel C, Messina-Graham S, Moh A, et al. Mouse hematopoietic cell-targeted STAT3 deletion: stem/progenitor cell defects, mitochondrial dysfunction, ROS overproduction, and a rapid aging-like phenotype. Blood (2012) 120:2589–2599. doi: 10.1182/blood-2012-01-404004
124. 124. Jenkins BJ, Roberts AW, Najdovska M, Grail D, Ernst M. The threshold of gp130-dependent STAT3 signaling is critical for normal regulation of hematopoiesis. Blood (2005) 105:3512–3520. doi:10.1182/blood-2004-09-3751
125. 125. Kato Y, Iwama A, Tadokoro Y, et al. Selective activation of STAT5 unveils its role in stem cell self-renewal in normal and leukemic hematopoiesis. J Exp Med (2005) 202:169–179. doi: 10.1084/jem.20042541
126. 126. Liao P, Wang W, Wang W, et al. CD8+ T cells and fatty acids orchestrate tumor ferroptosis and immunity via ACSL4. Cancer Cell (2022) 40:365–378.e6. doi: 10.1016/j.ccell.2022.02.003

© 2026 by the author(s). Distributed under a Creative Commons CC BY license.

Preprints.org (www.preprints.org) | NOT PEER-REVIEWED | Posted: 15 April 2026 doi:10.20944/preprints202604.0868.v2

127. 127. Lin Z, Zou S, Wen K. The crosstalk of CD8+ T cells and ferroptosis in cancer. Front Immunol (2023) 14:1255443. doi:10.3389/fimmu.2023.1255443
128. 128. Flem-Karlsen K, Talty R, McGeary MK, et al. Cytotoxic CD8+ T cells downregulate GPX4 to promote ferroptosis in melanoma that drives antitumor immunity. Cancer Res (2025) doi: 10.1158/0008-5472.CAN-24-1952
129. 129. Onodera A, González-Avalos E, Lio CJ, et al. Roles of TET and TDG in DNA demethylation in proliferating and non-proliferating immune cells. Genome Biol (2021) 22:186. doi: 10.1186/s13059-021-02384-1
130. 130. Blander JM, Medzhitov R. Toll-dependent selection of microbial antigens for presentation by dendritic cells. Nature (2006) 440:808–812. doi: 10.1038/nature04596
131. 131. Leonard JP, Sherman ML, Fisher GL, et al. Effects of single-dose interleukin-12 exposure on interleukin-12-associated toxicity and interferon-gamma production. Blood (1997) 90:2541–2548.
132. 132. Yoshida Y, Yoshimi R, Yoshii H, et al. The transcription factor IRF8 activates integrin-mediated TGF-beta signaling and promotes neuroinflammation. Immunity (2014) 40:187–198. doi:10.1016/j.immuni.2013.11.022
133. 133. Khan O, Giles JR, McDonald S, et al. TOX transcriptionally and epigenetically programs CD8+ T cell exhaustion. Nature (2019) 571:211–218. doi: 10.1038/s41586-019-1325-x
134. 134. Tucker CG, Mitchell JS, Martinov T, et al. Adoptive T cell therapy with IL-12-preconditioned low-avidity T cells prevents exhaustion and results in enhanced T cell activation, enhanced tumor clearance, and decreased risk for autoimmunity. J Immunol (2020) 205:1449–1460. doi:10.4049/jimmunol.2000007
135. 135. Grassmann S, Santosa EK, Kim H, et al. Stepwise epigenetic signal integration drives adaptive programming of cytotoxic lymphocytes. Immunity (2026) doi: 10.1016/j.immuni.2026.01.004
136. 136. Hajishengallis G, Chavakis T. Inflammageing and clonal haematopoiesis interplay and their impact on human disease. Nat Rev Mol Cell Biol (2026) doi: 10.1038/s41580-025-00936-y
137. 137. Mohammadnia N, Xue L, Vestjens LTW, et al. Colchicine and longitudinal dynamics of clonal hematopoiesis: an exploratory substudy of the LoDoCo2 trial. J Am Coll Cardiol (2025) 86:1983–1996. doi:10.1016/j.jacc.2025.08.025
138. 138. Wang D, Kaniowski D, Jacek K, et al. Bi-functional CpG-STAT3 decoy oligonucleotide triggers multilineage differentiation of acute myeloid leukemia in mice. Mol Ther Nucleic Acids (2024) 35:102268. doi:10.1016/j.omtn.2024.102268
139. 139. Soyano A, Lee MC, Han HS, et al. Intratumoral dendritic cell immunotherapy controls dissemination of metastasis-initiating cancer cells, even in patients with metastatic breast cancer. J Immunother Cancer (2026) 14:e013590. doi: 10.1136/jitc-2025-013590
140. 140. Daman AW, Antonelli AC, Redelman-Sidi G, et al. Microbial cancer immunotherapy reprograms hematopoiesis to enhance myeloid-driven anti-tumor immunity. Cancer Cell (2025) doi: 10.1016/j.ccell.2025.05.002
141. 141. Grajales-Reyes GE, Iwata A, Albring J, et al. Batf3 maintains autoactivation of Irf8 for commitment of a CD8α+ conventional DC clonogenic progenitor. Nat Immunol (2015) 16:708–717. doi:10.1038/ni.3197
142. 142. Matteini F, Thambyrajah R, Montserrat-Vazquez S, et al. A Notch trans-activation to cis-inhibition switch underlies hematopoietic stem cell aging. Blood (2025) doi: 10.1182/blood.2024026505
143. 143. You Z, Chi Y, Wang L, et al. Mitochondrial fitness controls cDC1-mediated antitumor immunity. Science (2026) 392:eadv6582. doi:10.1126/science.adv6582
144. 144. Molina IS, Haldar M. Mitochondria power immunity against cancer. Science (2026) 392:24–25. doi: 10.1126/science.aeg4325
145. 145. Du X, Wen J, Wang Y, et al. Hippo/Mst signalling couples metabolic state and immune function of CD8-alpha-positive dendritic cells. Nature (2018) 558:141–145. doi: 10.1038/s41586-018-0177-0
146. 146. Krawczyk CM, Holowka T, Sun J, et al. Toll-like receptor-induced changes in glycolytic metabolism regulate dendritic cell activation. Blood (2010) 115:4742–4749. doi: 10.1182/blood-2009-10-249540
147. 147. Tahiliani M, Koh KP, Shen Y, et al. Conversion of 5-methylcytosine to 5-hydroxymethylcytosine in mammalian DNA by MLL partner TET1. Science (2009) 324:930–935. doi: 10.1126/science.1170116

© 2026 by the author(s). Distributed under a Creative Commons CC BY license.

Preprints.org (www.preprints.org) | NOT PEER-REVIEWED | Posted: 15 April 2026 doi:10.20944/preprints202604.0868.v2

148. 148. Xiao M, Yang H, Xu W, et al. Inhibition of alpha-KG-dependent histone and DNA demethylases by fumarate and succinate that are accumulated in mutations of FH and SDH tumor suppressors. Genes Dev (2012) 26:1326–1338. doi: 10.1101/gad.191056.112
149. 149. Liu PS, Wang H, Li X, et al. Alpha-ketoglutarate orchestrates macrophage activation through metabolic and epigenetic reprogramming. Nat Immunol (2017) 18:985–994. doi: 10.1038/ni.3796
150. 150. Zhou B, Magana L, Hong Z, et al. The angiocrine Rspondin3 instructs interstitial macrophage transition via metabolic-epigenetic reprogramming and resolves inflammatory injury. Nat Immunol (2020) 21:1430–1443. doi: 10.1038/s41590-020-0764-8
151. 151. Nie Y, Erion DM, Yuan Z, et al. STAT3 inhibition of gluconeogenesis is downregulated by SirT1. Nat Cell Biol (2009) 11:492–500. doi:10.1038/ncb1857
152. 152. Limagne E, Thibaudin M, Euvrard R, et al. Sirtuin-1 activation controls tumor growth by impeding Th17 differentiation via STAT3 deacetylation. Cell Rep (2017) 19:746–759. doi:10.1016/j.celrep.2017.04.004
153. 153. Gomes AP, Price NL, Ling AJY, et al. Declining NAD+ induces a pseudohypoxic state disrupting nuclear-mitochondrial communication during aging. Cell (2013) 155:1624–1638. doi: 10.1016/j.cell.2013.11.037
154. 154. Everts B, Amiel E, Huang SC, et al. TLR-driven early glycolytic reprogramming via the kinases TBK1-IKK-epsilon supports the anabolic demands of dendritic cell activation. Nat Immunol (2014) 15:323–332. doi: 10.1038/ni.2833
155. 155. Ugele I, Cardenas-Conejo ZE, Gessner A, et al. D-2-hydroxyglutarate and L-2-hydroxyglutarate inhibit IL-12 secretion by human monocyte-derived dendritic cells. Int J Mol Sci (2019) 20:742. doi:10.3390/ijms20030742
156. 156. Hammon K, Renner K, Kreutz M, et al. D-2-hydroxyglutarate supports a tolerogenic phenotype with lowered major histocompatibility class II expression in non-malignant dendritic cells and acute myeloid leukemia cells. Haematologica (2024) 109:2500–2514. doi:10.3324/haematol.2023.283597
157. 157. Tian Y, Machado HB, Bhatt DL, et al. IFN-gamma regulates NAD+ metabolism to promote the respiratory burst in human monocytes. Blood Adv (2022) 6:3821–3834. doi: 10.1182/bloodadvances.2022007839
158. 158. Wölfle SJ, Strebovsky J, Bartz H, et al. PD-L1 expression on tolerogenic APCs is controlled by STAT-3. Eur J Immunol (2011) 41:413–424. doi: 10.1002/eji.201040979
159. 159. Zerdes I, Wallerius M, Sifakis EG, et al. STAT3 activity promotes programmed-death ligand 1 expression and suppresses immune responses in breast cancer. Cancers (2019) 11:E1479. doi: 10.3390/cancers11101479
160. 160. Bu LL, Yu GT, Wu L, et al. STAT3 induces immunosuppression by upregulating PD-1/PD-L1 in HNSCC. J Dent Res (2017) 96:1027–1034. doi:10.1177/0022034517712435
161. 161. Zhang B, Xu A, Wang H, et al. MPC-mediated lactate production drives histone lactylation in dendritic cells to affect tumor progression and immunotherapy. Cell Mol Life Sci (2025) 82:371. doi:10.1007/s00018-025-05881-9
162. 162. Sun K, Zhang X, Shi J, et al. Elevated protein lactylation promotes immunosuppressive microenvironment and therapeutic resistance in pancreatic ductal adenocarcinoma. J Clin Invest (2025) 135:e187024. doi:10.1172/JCI187024
163. 163. Doolittle ML, et al. Aged murine bone marrow myeloid and mesenchymal cells develop unique senescence phenotypes. J Clin Invest (2026) 136:e195772. doi: 10.1172/JCI195772
164. 164. Hofbauer LC, Rauner M. Deconstructing senescence phenotypes in cells of the bone and bone marrow. J Clin Invest (2026) 136:e204645. doi: 10.1172/JCI204645
165. 165. Sladitschek-Martens HL, et al. YAP/TAZ activity in stromal cells prevents ageing by controlling cGAS-STING. Nature (2022) 607:790–798. doi: 10.1038/s41586-022-04924-6
166. 166. Ambrosi TH, et al. Aged skeletal stem cells generate an inflammatory degenerative niche. Nature (2021) 597:256–262. doi:10.1038/s41586-021-03795-7
167. 167. Mitchell CA, et al. Stromal niche inflammation mediated by IL-1 signaling is a targetable driver of hematopoietic aging. Cell Stem Cell (2023) 30:820–837. doi: 10.1016/j.stem.2023.05.006

© 2026 by the author(s). Distributed under a Creative Commons CC BY license.

Preprints.org (www.preprints.org) | NOT PEER-REVIEWED | Posted: 15 April 2026 doi:10.20944/preprints202604.0868.v2

168. 168. Molina CM, Haldar M. Mitochondrial metabolism and signaling direct dendritic cell function in antitumor immunity. Science (2026) 387:eadv6582. doi: 10.1126/science.adv6582
169. 169. Kim TW, et al. IL-6 selectively suppresses cDC1 specification via C/EBP-beta. J Exp Med (2023) 220:e20230235. doi: 10.1084/jem.20230235
170. 170. Luo Y, et al. Senolytic drugs dasatinib and quercetin promote skin papilloma progression by eliminating senescent cells and impairing immune surveillance. One Health Adv (2025) 3:5. doi:10.26599/OSHM.2025.9610005
171. 171. Patel SB, et al. STAT3 protects hematopoietic stem cells by preventing activation of a deleterious autocrine type-I interferon response. Leukemia (2024) 38:1707–1721. doi: 10.1038/s41375-024-02218-6
172. 172. Friedrich MJ, et al. Transient hepatic reconstitution of trophic factors enhances aged immunity. Nature (2025) 639:756–764. doi:10.1038/s41586-025-09873-4
173. 173. Ross JB, et al. Depleting myeloid-biased haematopoietic stem cells rejuvenates aged immunity. Nature (2024) 628:162–170. doi:10.1038/s41586-024-07238-x
174. 174. Gadecka A, et al. The senolytic cocktail, dasatinib and quercetin, impacts the chromatin structure of both young and senescent vascular smooth muscle cells. GeroScience (2025) 47:1299–1315. doi:10.1007/s11357-024-01504-6
175. 175. Fang C, Qiao Y, Mun SH, et al. Cutting edge: EZH2 promotes osteoclastogenesis by epigenetic silencing of the negative regulator IRF8. J Immunol (2016) 196:4452–4456. doi: 10.4049/jimmunol.1501466
176. 176. Pan YM, Wang CG, Zhu M, et al. STAT3 signaling drives EZH2 transcriptional activation and mediates poor prognosis in gastric cancer. Mol Cancer (2016) 15:79. doi: 10.1186/s12943-016-0561-z
177. 177. Kim D, Park G, Huuhtanen J, et al. STAT3 activation in large granular lymphocyte leukemia is associated with cytokine signaling and DNA hypermethylation. Leukemia (2021) 35:3430–3443. doi:10.1038/s41375-021-01296-0
178. 178. Dasgupta M, Dermawan JK, Willard B, Stark GR. STAT3-driven transcription depends upon the dimethylation of K49 by EZH2. Proc Natl Acad Sci USA (2015) 112:3985–3990. doi: 10.1073/pnas.1503152112
179. 179. Kim E, Kim M, Woo DH, et al. Phosphorylation of EZH2 activates STAT3 signaling via STAT3 methylation and promotes tumorigenicity of glioblastoma stem-like cells. Cancer Cell (2013) 23:839–852. doi:10.1016/j.ccr.2013.04.008
180. 180. Beerman I, Bock C, Garrison BS, et al. Proliferation-dependent alterations of the DNA methylation landscape underlie hematopoietic stem cell aging. Cell Stem Cell (2013) 12:413–425. doi:10.1016/j.stem.2013.01.017
181. 181. Wen H, Dou Y, Hogaboam CM, Kunkel SL. Epigenetic regulation of dendritic cell-derived interleukin-12 facilitates immunosuppression after a severe innate immune response. Blood (2008) 111:1797–1804. doi:10.1182/blood-2007-08-106443
182. 182. DiNardo AR, Netea MG, Musher DM. Postinfectious epigenetic immune modifications—a double-edged sword. N Engl J Med (2021) 384:261–270. doi: 10.1056/NEJMra2028358
183. 183. Zhan Y, Zhang Y, Zhang S, et al. Differential requirement for the polycomb repressor complex 2 in dendritic cell and tissue-resident myeloid cell homeostasis. Sci Immunol (2021) 6:eabf7268. doi:10.1126/sciimmunol.abf7268
184. 184. Huang S, Wang Z, Zhou J, et al. EZH2 inhibitor GSK126 suppresses antitumor immunity by driving production of myeloid-derived suppressor cells. Cancer Res (2019) 79:2009–2020. doi:10.1158/0008-5472.CAN-18-2395
185. 185. Qiang N, Ao J, Nakamura M, et al. Alteration of the tumor microenvironment by pharmacological inhibition of EZH2 in hepatocellular carcinoma. Int Immunopharmacol (2023) 118:110068. doi:10.1016/j.intimp.2023.110068
186. 186. Chibaya L, Murphy KC, DeMarco KD, et al. EZH2 inhibition remodels the inflammatory senescence-associated secretory phenotype to potentiate pancreatic cancer immune surveillance. Nat Cancer (2023) 4:872–892. doi:10.1038/s43018-023-00553-8
187. 187. Sun D, Luo M, Jeong M, et al. Epigenomic profiling of young and aged HSCs reveals concerted changes during aging that reinforce self-renewal. Cell Stem Cell (2014) 14:673–688. doi:10.1016/j.stem.2014.03.002

© 2026 by the author(s). Distributed under a Creative Commons CC BY license.

Preprints.org (www.preprints.org) | NOT PEER-REVIEWED | Posted: 15 April 2026 doi:10.20944/preprints202604.0868.v2

188. 188. Kuribayashi W, Tanaka-Yano M, Park B, et al. Age-like methylation changes of HSCs in GADD45B knockout mice define methylation sites associated with loss of function. Aging Cell (2026) 25:e70453. doi:10.1111/acel.70453
189. 189. Adelman ER, Huang HT, Roisman A, et al. Aging human hematopoietic stem cells manifest profound epigenetic reprogramming of enhancers that may predispose to leukemia. Cancer Discov (2019) 9:1080–1101. doi:10.1158/2159-8290.CD-18-1474
190. 190. Flohr Svendsen A, Yang D, Kim K, et al. A comprehensive transcriptome signature of murine hematopoietic stem cell aging. Blood (2021) 138:439–451. doi: 10.1182/blood.2020009729
191. 191. Williams O, Hu L, Huang W, et al. Nore1 inhibits age-associated myeloid lineage skewing and clonal hematopoiesis but facilitates termination of emergency (stress) granulopoiesis. J Biol Chem (2023) 299:104867. doi: 10.1016/j.jbc.2023.104867
192. 192. De Santa F, Totaro MG, Prosperini E, et al. The histone H3 lysine-27 demethylase Jmjd3 links inflammation to inhibition of polycomb-mediated gene silencing. Cell (2007) 130:1083–1094. doi:10.1016/j.cell.2007.08.019
193. 193. Yıldırım-Buharalıoğlu G, Bond M, Sala-Newby GB, et al. Regulation of epigenetic modifiers, including KDM6B, by interferon-gamma and interleukin-4 in human macrophages. Front Immunol (2017) 8:92. doi:10.3389/fimmu.2017.00092
194. 194. Mikulski P, Tehrani SSH, Kogan A, et al. Heritable maintenance of chromatin modifications confers transcriptional memory of interferon-gamma signaling. Nat Struct Mol Biol (2025). doi:10.1038/s41594-025-01522-8
195. 195. Ovadya Y, Landsberger T, Leins H, et al. Impaired immune surveillance accelerates accumulation of senescent cells and aging. Nat Commun (2018) 9:5435. doi: 10.1038/s41467-018-07825-3
196. 196. Antonangeli F, Zingoni A, Soriani A, Santoni A. Senescent cells: living or dying is a matter of NK cells. J Leukoc Biol (2019) 105:1275–1283. doi: 10.1002/JLB.MR0718-299R
197. 197. Waight JD, Netherby C, Hensen ML, et al. Myeloid-derived suppressor cell development is regulated by a STAT/IRF-8 axis. J Clin Invest (2013) 123:4464–4478. doi: 10.1172/JCI68189
198. 198. Harroch S, Gothelf Y, Watanabe N, Revel M, Chebath J. Interleukin-6 activates and regulates transcription factors of the interferon regulatory factor family in M1 cells. J Biol Chem (1993) 268:9092–9097
199. 199. Orabona C, Puccetti P, Vacca C, et al. Toward the identification of a tolerogenic signature in IDO-competent dendritic cells. Blood (2006) 107:2846–2854. doi: 10.1182/blood-2005-10-4077
200. 200. Gargaro M, Scalisi G, Manni G, et al. Indoleamine 2,3-dioxygenase 1 activation in mature cDC1 promotes tolerogenic education of inflammatory cDC2 via metabolic communication. Immunity (2022) 55:1032–1050.e14. doi:10.1016/j.immuni.2022.05.013
201. 201. Ye ZH, Jiang XM, Huang MY, et al. Regulation of CD47 expression by interferon-gamma in cancer cells. Transl Oncol (2021) 14:101162. doi:10.1016/j.tranon.2021.101162
202. 202. Hendriks MAJM, Britsch I, Ke X, et al. Cancer cells under immune attack acquire CD47-mediated adaptive immune resistance independent of the myeloid CD47-SIRPα axis. Oncoimmunology (2021) 10:2005344. doi:10.1080/2162402X.2021.2005344
203. 203. Xu MM, Pu Y, Han D, et al. Dendritic cells but not macrophages sense tumor mitochondrial DNA for cross-priming through signal regulatory protein α signaling. Immunity (2017) 47:363–373.e5. doi:10.1016/j.immuni.2017.07.016
204. 204. Santarelli R, Gonnella R, Di Giovenale G, et al. STAT3 activation by KSHV correlates with IL-10, IL-6 and IL-23 release and an autophagic block in dendritic cells. Sci Rep (2014) 4:4241. doi: 10.1038/srep04241
205. 205. Masztalerz A, Van Rooijen N, Den Otter W, Everse LA. Mechanisms of macrophage cytotoxicity in IL-2 and IL-12 mediated tumour regression. Cancer Immunol Immunother (2003) 52:235–242. doi:10.1007/s00262-003-0381-z
206. 206. Yokogami K, Wakisaka S, Avruch J, Reeves SA. Serine phosphorylation and maximal activation of STAT3 during CNTF signaling is mediated by the rapamycin target mTOR. Curr Biol (2000) 10:47–50. doi:10.1016/s0960-9822(99)00268-7

© 2026 by the author(s). Distributed under a Creative Commons CC BY license.

Preprints.org (www.preprints.org) | NOT PEER-REVIEWED | Posted: 15 April 2026 doi:10.20944/preprints202604.0868.v2

207. 207. Pinno J, Bongartz H, Klepsch O, et al. Interleukin-6 influences stress-signalling by reducing the expression of the mTOR-inhibitor REDD1 in a STAT3-dependent manner. Cell Signal (2016) 28:907–916. doi:10.1016/j.cellsig.2016.04.004
208. 208. Weichhart T, Costantino G, Poglitsch M, et al. The TSC-mTOR signaling pathway regulates the innate inflammatory response. Immunity (2008) 29:565–577. doi: 10.1016/j.immuni.2008.08.012
209. 209. Braun M, Ress ML, Yoo YE, et al. IL12-mediated sensitizing of T-cell receptor-dependent and -independent tumor cell killing. Oncoimmunology (2016) 5:e1188245. doi: 10.1080/2162402X.2016.1188245
210. 210. Derré L, Corvaisier M, Pandolfino MC, et al. Expression of CD94/NKG2-A on human T lymphocytes is induced by IL-12: implications for adoptive immunotherapy. J Immunol (2002) 168:4864–4870. doi:10.4049/jimmunol.168.10.4864
211. 211. Vom Berg J, Prokop S, Miller KR, et al. Inhibition of IL-12/IL-23 signaling reduces Alzheimer's disease-like pathology and cognitive decline. Nat Med (2012) 18:1812–1819. doi: 10.1038/nm.2965
212. 212. Schneeberger S, Kim SJ, Geesdorf MN, et al. Interleukin-12 signaling drives Alzheimer's disease pathology through disrupting neuronal and oligodendrocyte homeostasis. Nat Aging (2025) 5:622–641. doi:10.1038/s43587-025-00816-2
213. 213. Li H, Bullock K, Gurber C, et al. Metabolomic adaptations and correlates of survival to immune checkpoint blockade. Nat Commun (2019) 10:4346. doi: 10.1038/s41467-019-12361-9
214. 214. Zhang C, Chien C, Jurgaitytė E, et al. Intratumoral Treg cell ablation elicits NK cell-mediated control of CD8 T cell-resistant tumors. Sci Immunol (2026). doi: 10.1126/sciimmunol.adx4411
215. 215. Tsui KH, Cheng SH, Wang B, et al. Mitochondrial quality control as a central pharmacological target in aging. Pharmacol Res (2026) 227:108188. doi: 10.1016/j.phrs.2025.108188
216. 216. Wang W, Hu Y, Yang C, et al. Decreased NAD activates STAT3 and integrin pathways to drive epithelial-mesenchymal transition. Mol Cell Proteomics (2018) 17:2005–2017. doi: 10.1074/mcp.RA118.000882
217. 217. Minhas PS, Liu L, Moon PK, et al. Macrophage de novo NAD synthesis specifies immune function in aging and inflammation. Nat Immunol (2019) 20:50–63. doi: 10.1038/s41590-018-0255-3
218. 218. O'Hagan HM, Mohammad HP, Baylin SB. Double strand breaks can initiate gene silencing and SIRT1-dependent onset of DNA methylation in an exogenous promoter CpG island. PLoS Genet (2008) 4:e1000155. doi:10.1371/journal.pgen.1000155
219. 219. Pruitt K, Zinn RL, Ohm JE, et al. Inhibition of SIRT1 reactivates silenced cancer genes without loss of promoter DNA hypermethylation. PLoS Genet (2006) 2:e40. doi: 10.1371/journal.pgen.0020040
220. 220. Petrocelli JJ, McKenzie AI, de Hart NMMP, et al. Disuse-induced muscle fibrosis, cellular senescence, and senescence-associated secretory phenotype in older adults are alleviated during re-ambulation with metformin pre-treatment. Aging Cell (2023) 22:e13936. doi:10.1111/acel.13936
221. 221. Vasamsetti SB, Karnewar S, Kanugula AK, et al. Metformin inhibits monocyte-to-macrophage differentiation via AMPK-mediated inhibition of STAT3 activation. Diabetes (2015) 64:2028–2041. doi: 10.2337/db14-1225
222. 222. Khan J, Pernicova I, Nisar K, Korbonits M. Mechanisms of ageing: growth hormone, dietary restriction, and metformin. Lancet Diabetes Endocrinol (2023) 11:261–281. doi: 10.1016/S2213-8587(23)00001-3
223. 223. Liu X, Yu P, Xu Y, et al. Metformin induces tolerogenicity of dendritic cells by promoting metabolic reprogramming. Cell Mol Life Sci (2023) 80:283. doi: 10.1007/s00018-023-04932-3
224. 224. Lee WJ, Zhu BT. Inhibition of DNA methylation by caffeic acid and chlorogenic acid, two common catechol-containing coffee polyphenols. Carcinogenesis (2006) 27:269–277. doi: 10.1093/carcin/bgi206
225. 225. Legaz A, Moguilner S, Barttfeld P, et al. The exposome of brain aging across 34 countries. Nat Med (2026). doi:10.1038/s41591-026-04302-z
226. 226. Tang Q, Fang J, Lai W, et al. Hippo pathway monomerizes STAT3 to regulate prostate cancer growth. Cancer Sci (2022) 113:2753–2762. doi: 10.1111/cas.15463
227. 227. Hopwood TW, Hall S, Begley N, et al. The circadian regulator BMAL1 programmes responses to parasitic worm infection via a dendritic cell clock. Sci Rep (2018) 8:3782. doi:10.1038/s41598-018-22021-5

© 2026 by the author(s). Distributed under a Creative Commons CC BY license.

Preprints.org (www.preprints.org) | NOT PEER-REVIEWED | Posted: 15 April 2026 doi:10.20944/preprints202604.0868.v2

228. 228. Cervantes-Silva MP, Carroll RG, Wilk MM, et al. The circadian clock influences T cell responses to vaccination by regulating dendritic cell antigen processing. Nat Commun (2022) 13:7217. doi:10.1038/s41467-022-34897-z
229. 229. Manicassamy S, Reizis B, Ravindran R, et al. Activation of beta-catenin in dendritic cells regulates immunity versus tolerance in the intestine. Science (2010) 329:849–853. doi:10.1126/science.1188510
230. 230. Sheen JH, Strainic MG, Liu J, et al. TLR-induced murine dendritic cell (DC) activation requires DC-intrinsic complement. J Immunol (2017) 199:278–291. doi: 10.4049/jimmunol.1700339
231. 231. Gargaro M, Vacca C, Massari S, et al. Engagement of nuclear coactivator 7 by 3-hydroxyanthranilic acid enhances activation of aryl hydrocarbon receptor in immunoregulatory dendritic cells. Front Immunol (2019) 10:1973. doi: 10.3389/fimmu.2019.01973
232. 232. Zhao Y, Shen X, Na N, et al. mTOR masters monocyte development in bone marrow by decreasing the inhibition of STAT5 on IRF8. Blood (2018) 131:1587–1599. doi: 10.1182/blood-2017-04-777128
233. 233. Wiernicki B, Maschalidi S, Pinney J, et al. Cancer cells dying from ferroptosis impede dendritic cell-mediated anti-tumor immunity. Nat Commun (2022) 13:3676. doi: 10.1038/s41467-022-31218-2
234. 234. Han L, Bai L, Qu C, et al. PPARG-mediated ferroptosis in dendritic cells limits antitumor immunity. Biochem Biophys Res Commun (2021) 576:33–39. doi: 10.1016/j.bbrc.2021.08.082
235. 235. Schaupp L, Muth S, Rogell L, et al. Microbiota-induced type I interferons instruct a poised basal state of dendritic cells. Cell (2020) 181:1080–1096. doi: 10.1016/j.cell.2020.04.022
236. 236. Ocaña-Morgner C, Neutral sphingomyelinase and ceramide in dendritic cell activation and IL-12 production during immune responses. J Immunol (2007) 178:6741–6751.
237. 237. Novitskiy SV, Ryzhov S, Zaynagetdinov R, et al. Adenosine receptors in regulation of dendritic cell differentiation and function. Blood (2008) 112:1822–1831. doi: 10.1182/blood-2008-02-136325
238. 238. Kalinski P, Vieira PL, Schuitemaker JH, de Jong EC, Kapsenberg ML. Prostaglandin E(2) is a selective inducer of interleukin-12 p40 (IL-12p40) production and an inhibitor of bioactive IL-12p70 heterodimer. Blood (2001) 97:3466–3469. doi: 10.1182/blood.v97.11.3466
239. 239. Kalinski P, Schuitemaker JH, Hilkens CM, Kapsenberg ML. Prostaglandin E2 induces the final maturation of IL-12-deficient CD1a+CD83+ dendritic cells: the levels of IL-12 are determined during the final dendritic cell maturation and are resistant to further modulation. J Immunol (1998) 161:2804–2809.
240. 240. Khayrullina T, Yen JH, Jing H, Ganea D. In vitro differentiation of dendritic cells in the presence of prostaglandin E2 alters the IL-12/IL-23 balance and promotes differentiation of Th17 cells. J Immunol (2008) 181:721–735. doi: 10.4049/jimmunol.181.1.721
241. 241. Van Elssen CH, Vanderlocht J, Oth T, et al. Inflammation-restraining effects of prostaglandin E2 on natural killer-dendritic cell (NK-DC) interaction are imprinted during DC maturation. Blood (2011) 118:2473–2482. doi: 10.1182/blood-2010-09-307835
242. 242. Bayerl F, Meiser P, Donakonda S, et al. Tumor-derived prostaglandin E2 programs cDC1 dysfunction to impair intratumoral orchestration of anti-cancer T cell responses. Immunity (2023) 56:1341–1358.e11. doi: 10.1016/j.immuni.2023.05.011
243. 243. Anguille S, Smits EL, Lion E, van Tendeloo VF, Berneman ZN. Clinical use of dendritic cells for cancer therapy. Lancet Oncol (2014) 15:e257–e267. doi: 10.1016/S1470-2045(13)70585-0
244. 244. Li Y, Jia X, Liu M, et al. Impact of NSAID type, initiation timing, duration and dose on clinical outcomes of immunotherapy in NSCLC: a multicenter two-cohort study. J Immunother Cancer (2026) 14:e014360. doi: 10.1136/jitc-2025-014360
245. 245. Punyawatthananukool S, Matsuura R, Wongchang T, et al. Prostaglandin E2-Ep2/Ep4 signaling induces immunosuppression in human cancer by impairing bioenergetics and ribosome biogenesis in immune cells. Nat Commun (2024) 15:9464. doi: 10.1038/s41467-024-53706-3
246. 246. Jang C, Chen L, Rabinowitz JD. Metabolomics and isotope tracing. Cell (2018) 173:822–837. doi: 10.1016/j.cell.2018.03.055
247. 247. Kaya-Okur HS, Wu SJ, Codomo CA, et al. CUT&Tag for efficient epigenomic profiling of small samples and single cells. Nat Commun (2019) 10:1930. doi: 10.1038/s41467-019-09982-5
248. 248. Fahy GM, Brooke RT, Watson JP, et al. Reversal of epigenetic aging and immunosenescent trends in humans. Aging Cell (2019) 18:e13028. doi: 10.1111/acel.13028

© 2026 by the author(s). Distributed under a Creative Commons CC BY license.

Preprints.org (www.preprints.org) | NOT PEER-REVIEWED | Posted: 15 April 2026 doi:10.20944/preprints202604.0868.v2

249. 249. Li B, Peng X, Li H, et al. Single-cell immune aging clocks reveal inter-individual heterogeneity during infection and vaccination. Nat Aging (2025) 5:635–651. doi: 10.1038/s43587-025-00819-z
250. 250. Kantoff PW, Higano CS, Shore ND, et al. Sipuleucel-T immunotherapy for castration-resistant prostate cancer. N Engl J Med (2010) 363:411–422. doi: 10.1056/NEJMoa1001294
251. 251. Yamamoto K, Shibata F, Miyasaka N, Miura O. The human perforin gene is a direct target of STAT4 activated by IL-12 in NK cells. Biochem Biophys Res Commun (2002) 297:1245–1252. doi: 10.1016/s0006-291x(02)02378-1
252. 252. Hazeldine J, Hampson P, Lord JM. Reduced release and binding of perforin at the immunological synapse underlies the age-related decline in natural killer cell cytotoxicity. Aging Cell (2012) 11:751–759. doi: 10.1111/j.1474-9726.2012.00839.x
253. 253. Koroma AK, Singh K, Wang Y, et al. Overactivation of Cdc42 GTPase impairs the cytotoxic function of NK cells from old individuals towards senescent fibroblasts. Aging Cell (2026) 25:e70398. doi: 10.1111/acel.70398
254. 254. Sagiv A, Biran A, Yon M, et al. Granule exocytosis mediates immune surveillance of senescent cells. Oncogene (2013) 32:1971–1977. doi: 10.1038/onc.2012.206
255. 255. Shehata HM, Hoebe K, Chougnet CA. The aged nonhematopoietic environment impairs natural killer cell maturation and function. Aging Cell (2015) 14:191–199. doi: 10.1111/acel.12303
256. 256. Chiu BC, Martin BE, Stolberg VR, Chensue SW. The host environment is responsible for aging-related functional NK cell deficiency. J Immunol (2013) 191:4688–4698. doi: 10.4049/jimmunol.1301625
257. 257. Bonnema JD, Rivlin KA, Ting AT, et al. Cytokine-enhanced NK cell-mediated cytotoxicity: positive modulatory effects of IL-2 and IL-12 on stimulus-dependent granule exocytosis. J Immunol (1994) 152:2098–2104.
258. 258. Nogusa S, Murasko DM, Gardner EM. Differential effects of stimulatory factors on natural killer cell activities of young and aged mice. J Gerontol A Biol Sci Med Sci (2012) 67:947–954. doi: 10.1093/gerona/gls079

Disclaimer/Publisher's Note: The statements, opinions and data contained in all publications are solely those of the individual author(s) and contributor(s) and not of MDPI and/or the editor(s). MDPI and/or the editor(s) disclaim responsibility for any injury to people or property resulting from any ideas, methods, instructions or products referred to in the content.

© 2026 by the author(s). Distributed under a Creative Commons CC BY license.